NATIONAL ADVISORY COMMITTEE FOR AERONAUTICS

NACA TECHNICAL NOTE 3792

A THEORETICAL ANALYSIS OF HEAT TRANSFER IN REGIONS OF SEPARATED FLOW

By Dean R. Chapman

Ames Aeronautical Laboratory
Moffett Field, Calif.

Washington
October 1956

NATIONAL ADVISORY COMMITTEE FOR AERONAUTICS

TECHNICAL NOTE 3792

A THEORETICAL ANALYSIS OF HEAT TRANSFER IN REGIONS OF SEPARATED FLOW

By Dean R. Chapman

SUMMARY

The flow field analyzed consists of a thin, constant pressure, viscous mixing layer separated from a solid surface by an enclosed region of low-velocity air ("dead air"). The law of conservation of energy is employed to relate calculated conditions within the separated mixing layer to the rate of heat transfer at the solid surface. This physical model is applied to laminar separations in compressible flow for various Prandtl numbers, including consideration of the case where air is injected into the separated region. Application to turbulent separations is made for a Prandtl number of unity in low-speed flow without injection. All calculations are for the case of zero boundary-layer thickness at the position of separation.

For laminar separations the differential equations for viscous flow at arbitrary Mach number are solved for the enthalpy and velocity profiles within the thin layer where mixing with dead air takes place. Results are presented in tabular form for Prandtl numbers between 0.1 and 10. The rate of heat transfer to a separated laminar region in air ($Pr = 0.72$) is calculated to be 0.56 of that to a corresponding attached laminar boundary layer having the same constant pressure. Injection of gas into the separated region is calculated to have a powerful effect in reducing the rate of heat transfer to the wall. It is calculated that a moderate quantity of gas injection reduces to zero the heat transfer in a laminar separated flow.

INTRODUCTION

Separated laminar layers (sometimes called "free layers") have long been known to be quite unstable in subsonic flow. A rule of thumb based on experiments of von Doenhoff (ref. 1) is that a separated laminar layer in subsonic flow will remain laminar downstream of separation only for a run of about 50,000 in Reynolds number (based on length along separated layer), after which transition occurs. Because of this low stability relative to attached laminar flows (which remain laminar to Reynolds numbers the order of 10^6), the special type of separated flow wherein a viscous layer remains laminar not only downstream of separation but also

for a short distance downstream of reattachment has occurred only rather rarely in the past. As a result, the "pure laminar" type of separated flow, which is the main subject for analysis in this report, formerly has been regarded primarily as a laboratory curiosity rather than a practical phenomenon.

Some interest recently has been stimulated in the pure laminar type of separated flow, inasmuch as free laminar layers appear to be surprisingly stable at hypersonic Mach numbers. It was observed in reference 2 that the stability of separated laminar layers increases markedly with an increase in Mach number until, at Mach numbers near 4, they can become for certain configurations almost as stable as an attached laminar boundary layer (laminar to about 1 million Reynolds number). This strong increase in stability makes separated laminar flows of practical interest, especially at hypersonic Mach numbers. The actual extent of this practicality, however, is not known at present inasmuch as the available data are meager above Mach numbers of about 4. The effect of cold-wall conditions on the stability of separated laminar flows is not known, nor is the effect of gas injection on stability known.

In view of the trend of increasing stability with increasing Mach numbers, it is pertinent to inquire into the heat-transfer characteristics of separated flows. It might be expected intuitively that the rate of heat transfer from a region of separated laminar flow would be smaller than that from a comparable attached laminar boundary layer. This expectation, in fact, led Stalder and Nielsen (ref. 3) to conduct experiments with separated flow induced by a probe in front of a blunt-nosed object. Instead of finding a lower heat-transfer rate when separation was induced, they observed a doubling in the heat-transfer rate. In retrospect, however, it has been concluded from a detailed examination of their original shadowgraphs that the separated flow induced by the probe was of the "transitional" type (transition between separation and reattachment), whereas the attached flow to which they made comparison was that of a completely laminar boundary layer. They compared a partly turbulent separated flow with a fully laminar attached flow. Hence, the question remains open as to whether a pure laminar separated flow has a higher or lower rate of heat transfer than a comparable attached laminar flow.

The main object of the present paper is to compare by means of theoretical calculation the heat-transfer rate in a separated laminar region with that of a corresponding attached laminar boundary layer. Secondary objectives are to consider the case of gas injection, and to apply the theoretical ideas also to turbulent separation. In a previous paper (ref. 4), the velocity profiles within a separated laminar mixing layer were calculated under the assumption that the specific heat was constant. In the present paper, calculations are made of the enthalpy profiles as well as the rate of heat transfer. The theory of reference 4 is extended to include the case where the specific heat is a function of temperature, since this case corresponds to conditions encountered in hypersonic flight.

NOTATION

b	width of two-dimensional flow
c_p	specific heat at constant pressure
C	constant of proportionality between viscosity and temperature
C_1	constant defined by equation (24)
F_1, F_2	functions defined by equations (23)
G	function defined by equation (22)
g_1, g_2	functions defined by equations (26)
h	enthalpy per unit mass
I_1, I_2	functions defined by equations (48) and (49)
l	length of separated mixing layer
m	mass flux (density $\times$ velocity $\times$ area)
M	Mach number
p	static pressure
Q_w	total heat flux to wall between separation and reattachment points
$\bar{q}_w$	average heat flux to wall per unit area, $\frac{Q_w}{\text{surface area}}$
r	recovery factor based on enthalpy (see eq. (42))
r_b	radius of base of cone
Re	Reynolds number based on conditions at outer edge of mixing layer and on length l
R	gas constant
Pr	Prandtl number
T	static temperature
u, v	local velocity components in x and y directions, respectively

x,y coordinates parallel and perpendicular, respectively, to direction of flow along dividing streamline ($\psi = 0$) within mixing layer

ρ mass density

μ viscosity

ψ stream function defined by equation (4)

ν kinematic viscosity, $\frac{\mu}{\rho}$

λ coefficient of heat conductivity

γ ratio of specific heats

ζ dimensionless mass-flow variable defined by equation (10)

η function defined by equation (15)

η_1,η_2 functions defined by equation (32)

Subscripts

a active degrees of freedom of molecule (translational and rotational)

d dead-air region

e outer edge of viscous layer

int internal degrees of freedom within molecule

i injected mass flow into separated region

o dividing stream line

t total conditions

w wall

* dimensionless quantities defined by equation (7)

bl boundary layer

Superscript

' ordinary differentiation

ANALYSIS

Physical Model

The type of separated flow analyzed is depicted schematically in figure 1. The pressure is regarded as essentially constant over the length l of the two-dimensional laminar mixing layer. Also, in accordance with the theoretical description advanced in reference 2, the region of recompression through the reattachment zone is assumed to be of small dimensions compared to l. This physical picture yields results consistent with the experiments of reference 2, in the sense that the dead-air pressure calculated according to such a physical picture agrees well with measurements for the case when reattachment occurs on an inclined plate. This establishes some confidence in the mechanism postulated, at least as a reasonable approximation.

The differential equations of momentum, continuity, and energy for viscous flow within the relatively thin, constant-pressure, laminar mixing layer are as follows:

$$\rho u \frac{\partial u}{\partial x} + \rho v \frac{\partial u}{\partial y} = \frac{\partial}{\partial y}\left(\mu \frac{\partial u}{\partial y}\right) \tag{1}$$

$$\frac{\partial(\rho u)}{\partial x} + \frac{\partial(\rho v)}{\partial y} = 0 \tag{2}$$

$$\rho u \frac{\partial h}{\partial x} + \rho v \frac{\partial h}{\partial y} = \frac{\partial}{\partial y}\left(\frac{\mu}{Pr} \frac{\partial h}{\partial y}\right) + \mu\left(\frac{\partial u}{\partial y}\right)^2 \tag{3}$$

The conditions at the outer edge of the mixing layer provide two boundary conditions: $u(x,\infty) = u_e$ and $h(x,\infty) = h_e$, where u_e and h_e are constants since the pressure is constant. The condition that dead air borders the low-velocity portion of the mixing layer provides two more boundary conditions: $u(x,-\infty) = 0$ and $h(x,-\infty) = h_w$. These latter two boundary conditions require some explanation since the mixing layer cannot extend to $-\infty$ due to the presence of the wall. Actually, the use of $-\infty$ in the boundary conditions means that the mixing-layer characteristics are determined as though the wall were an infinite distance away. It is assumed, in effect, then, that the presence of the wall distorts the mixing-layer profiles only to a minor degree in the region where the velocity is low. This will be a good assumption if the dimensions of the dead-air region are large compared to the mixing-layer thickness.

The above system of differential equations and boundary conditions is to be solved subject to the following additional assumptions:

(i) Pr = constant

(ii) $p = \rho RT$

(iii) $\mu/\mu_e = CT/T_e$

(iv) mixing-layer thickness at separation is 0 (or negligible compared to l)

Assumption (i) is a common one. Assumption (ii), taken together with thermodynamics theory, implies that the enthalpy is a function of temperature only. This allows the specific heat c_p to vary with the temperature as would be the case in hypersonic flight. Assumption (iii), introduced in reference 4, involves a constant C which is selected so that $\frac{\mu_{ref}}{\mu_e} = \frac{CT_{ref}}{T_e}$. If T_{ref} is selected as the wall temperature, and if Sutherland's equation for viscosity is employed, then $C = \sqrt{\frac{T_w}{T_e}} \frac{T_e + S}{T_w + S}$. Assumption (iv) is made to simplify the mathematical computations, since it implies that the profiles of velocity and enthalpy are similar at every station within the thin mixing layer. Brief discussion is presented later of how the analysis would be modified to consider the case of finite thickness of boundary layer at separation.

Transformation of Equations

The solution of equations (1) to (3) proceeds exactly the same as in references 4 and 5 by slightly modifying the von Mises transformation (ref. 6) as generalized to compressible flow by von Kármán and Tsien (ref. 7). The first step is to employ the stream function ψ as an independent variable, where

$$\rho u = \rho_e \frac{\partial \psi}{\partial y} \qquad \rho v = -\rho_e \frac{\partial \psi}{\partial x} \tag{4}$$

since this variable automatically satisfies the continuity equation (2). Transformation is made to (x_*, ψ_*) coordinates through the transformation formulae

$$\left(\frac{\partial}{\partial y}\right)_x = \frac{\rho u}{\rho_e} \left(\frac{\partial}{\partial \psi}\right)_x \tag{5}$$

$$\left(\frac{\partial}{\partial x}\right)_y = \frac{\rho v}{\rho_e} \left(\frac{\partial}{\partial \psi}\right)_x + \left(\frac{\partial}{\partial x}\right)_\psi \tag{6}$$

The following dimensionless variables are introduced:

$$\left.\begin{aligned} u_* &\equiv u/u_e \qquad h_* \equiv h/h_e \\ x_* &\equiv x/l \qquad \psi_* \equiv \psi/\sqrt{\nu_e u_e l C} \\ \rho_* &\equiv \rho/\rho_e \qquad \mu_* \equiv \mu/\mu_e = CT/T_e = CT_* \end{aligned}\right\} \tag{7}$$

When substituted into equations (1) and (3), the transformation formulae and dimensionless variables yield two basic equations

$$\frac{\partial u_*}{\partial x_*} = \frac{\partial}{\partial \psi_*}\left(u_* \frac{\partial u_*}{\partial \psi_*}\right) \tag{8}$$

$$\frac{\partial h_*}{\partial x_*} = \frac{1}{Pr}\frac{\partial}{\partial \psi_*}\left(u_* \frac{\partial h_*}{\partial \psi_*}\right) + \frac{u_e^2}{h_e} u_* \left(\frac{\partial u_*}{\partial \psi_*}\right)^2 \tag{9}$$

It is noted that neither the Mach number nor the ratio of specific heats γ appears in these equations. Only the ratio u_e^2/h_e appears. In the special case where T_e is low enough (less than about 700° R for air) so that no vibrational energy is excited within molecules, then $u_e^2/h_e = (\gamma_e - 1)M_e^2$. In the following, however, the form containing u_e^2/h_e is retained throughout.

A relatively simple solution of equations (8) and (9) is made possible since the momentum equation (eq. (8)) is independent of the energy equation (eq. (9)). The energy equation, however, is not independent of the momentum equation and, hence, the momentum equation must be solved first.

Solution of Momentum Equation

A solution of the momentum equation already has been obtained in reference 4. This solution corresponds to similar velocity profiles at each station along the mixing layer. The solution of reference 4 is given in terms of a single variable

$$\zeta \equiv \psi_*/\sqrt{x_*} \tag{10}$$

which reduces equation (8) to the ordinary differential equation

$$-\frac{\zeta}{2}\frac{du_*}{d\zeta} = \frac{d}{d\zeta}\left(u_* \frac{du_*}{d\zeta}\right) \tag{11}$$

Solution of this nonlinear differential equation, subject to the boundary conditions $u_*(\infty) = 1$ and $u_*(-\infty) = 0$, was obtained through the numerical procedure described in reference 4. The function $u_*(\zeta)$ is tabulated in table I.

A relation between ζ and the geometric coordinates (x,y) is required later in order to convert the $u_*(\zeta)$ function into physical velocity profiles $u_*(x,y)$. The appropriate relationship is derived from the stream-function differential

$$\frac{\rho u}{\rho_e} dy - \frac{\rho v}{\rho_e} dx = d\psi = \left(\frac{\partial \psi}{\partial \zeta}\right)_x d\zeta + \left(\frac{\partial \psi}{\partial x}\right)_\zeta dx$$

by considering a fixed value of x

$$\rho u \, dy = \rho_e \sqrt{\nu_e u_e l C} \, \frac{\partial \psi_*}{\partial \zeta} \, d\zeta = \rho_e \sqrt{\nu_e u_e x C} \, d\zeta \tag{12}$$

and then integrating

$$\frac{y}{2}\sqrt{\frac{u_e}{\nu_e x C}} = \frac{1}{2}\int_0^\zeta \frac{d\zeta}{\rho_* u_*} = \int_0^\zeta T_* \, \frac{d\zeta}{2u_*} \tag{13}$$

It is seen that even though the momentum equation is completely solved by the function $u_*(\zeta)$, actual velocity profiles cannot be calculated until the temperature function $T_*(\zeta)$ is calculated, as this function together with the $u_*(\zeta)$ function determines the relation between ζ and y.

The variable ζ is clearly a dimensionless mass-flow variable (see eq. (12)). Inasmuch as the mass flux m drawn out from the dead air by the scavenging action of the mixing layer up to station x must be finite,

$$\int_{-\infty}^{0} \rho u \, dy = \frac{m}{b} = \sqrt{\rho_e u_e \mu_e x C} \int_{\zeta=\zeta_d}^{\zeta=0} d\zeta = \text{finite}$$

$$= -\zeta_d \sqrt{\rho_e u_e \mu_e x C} \tag{14}$$

where ζ_d is the value of ζ at $u_* = 0$. Table I shows that $\zeta_d = -1.233$.

It is instructive, though not necessary to subsequent analysis, to digress temporarily in order to illustrate the relation between the

mass-flow variable ζ and the more familiar Blasius variable η where

$$\eta \equiv \frac{1}{2} \int_0^{\zeta} \frac{d\zeta}{u_*} \tag{15}$$

If a function $f(\eta)$ is employed as the dependent variable instead of the function $u_*(\zeta)$, a different differential equation is obtained in place of equation (11). By setting

$$f(\eta) \equiv \zeta \tag{16}$$

so that

$$\frac{1}{2} f'(\eta) = \frac{1}{2} \frac{d\zeta}{d\eta} = u_* \tag{17}$$

the differential equation becomes

$$f''' + ff'' = 0 \tag{18}$$

which is the familiar Blasius equation for incompressible, viscous, laminar flow over a flat plate. The boundary conditions to which equation (18) is subjected, however, are not the same as the familiar Blasius boundary conditions. The boundary conditions for a separated laminar mixing layer are

$$f'(\infty) = 2 \qquad f(0) = 0 \qquad f'(-\infty) = 0$$

The third of these boundary conditions differs from the corresponding boundary conditions in Blasius' problem, which would be $f'(0) = 0$. The relation between the function $f(\eta)$ and the function $u_*(\zeta)$ is given by equations (16), (17), and the relationship $f''(\eta) = 4u_* du_*/d\zeta$.

Solution of Energy Equation

Inasmuch as the variable ζ is pertinent to the solution of the momentum equation, the energy equation (9) also is transformed to (ζ, x_*) coordinates.

$$u_* \frac{\partial^2 h_*}{\partial \zeta^2} + \left(\Pr \frac{\zeta}{2} + \frac{du_*}{d\zeta} \right) \frac{\partial h_*}{\partial \zeta} - \Pr x_* \frac{\partial h_*}{\partial x_*} = -\Pr \frac{u_e^2}{h_e} u_* \left(\frac{du_*}{d\zeta} \right)^2 \tag{19}$$

This equation will be solved subject to the boundary condition $h(-\infty) \equiv h_w = \text{constant}$, which implies that the temperature of the dead air is constant just before it is drawn into the mixing layer. It is not known whether a constant temperature of this dead air can be realized in practice, inasmuch as appropriate experiments have not yet been conducted. The case $h_w = \text{constant}$, though, is relatively simple since the term involving $\partial/\partial x_*$ can be dropped from equation (19). If subsequent experiments show a variable "wall" enthalpy h_w to be essential, then equation (19) with the $\partial/\partial x_*$ term included would have to be solved in a manner analogous to the solution of reference 5. In the present analysis, however, it is assumed that $\partial h_*/\partial x_* = 0$, so that

$$u_* \frac{d^2 h_*}{d\zeta^2} + \left(\Pr \frac{\zeta}{2} + \frac{du_*}{d\zeta} \right) \frac{dh_*}{d\zeta} = -\Pr \frac{u_e^2}{h_e} u_* \left(\frac{du_*}{d\zeta} \right)^2 \tag{20}$$

This is a linear, second-order, ordinary differential equation, and is amenable to general solution. By noting from equation (11) that $u_* u_*'' + (u_*')^2 + \zeta u_*'/2 = 0$, the general solution to equation (20) can be written as

$$h_*(\zeta) = 1 + C_1 \int_\zeta^\infty (4u_* u_*')^{\Pr} \frac{d\zeta}{2u_*} + \frac{\Pr u_e^2}{4h_e} \int_\zeta^\infty (4u_* u_*')^{\Pr} G(\zeta) \frac{d\zeta}{2u_*} \tag{21}$$

where C_1 is an arbitrary constant to be evaluated from boundary conditions, and where

$$G(\zeta) \equiv \int_0^\zeta (4u_* u_*')^{2-\Pr} \frac{d\zeta}{2u_*} \tag{22}$$

Actually, the lower limit could, with equal generality, be an arbitrary number; zero is a convenient limit for reasons which will later appear. For convenience, the following two functions are introduced which will appear often in subsequent equations:

$$\left.\begin{aligned} F_1(\zeta) &\equiv \int_\zeta^\infty (4u_* u_*')^{\Pr} \frac{d\zeta}{2u_*} \\ F_2(\zeta) &\equiv \frac{\Pr}{2} \int_\zeta^\infty (4u_* u_*')^{\Pr} G(\zeta) \frac{d\zeta}{2u_*} \end{aligned}\right\} \tag{23}$$

The constant C_1 can now be written as

$$C_1 = \frac{\frac{h_w}{h_e} - 1 - \frac{u_e^2}{2h_e} F_2(\zeta_d)}{F_1(\zeta_d)} \tag{24}$$

where $F_1(\zeta_d)$ and $F_2(\zeta_d)$ depend only on the Prandtl number. Their values have been calculated from equations (23) and the known solution for $u_*(\zeta)$ as follows:

Pr	$F_1(\zeta_d)$	$F_2(\zeta_d)$
0.1	11.73	-0.202
.25	5.61	-.192
.5	3.40	-.178
.72	2.58	-.175
1.0	2.00	-.173
1.5	1.425	-.175
2.0	1.089	-.176
10.0	.079	-.204

The solution for enthalpy distribution becomes:

$$h_* \equiv \frac{h}{h_e} = 1 + \left(\frac{h_w}{h_e} - 1\right) g_1(\zeta) + \frac{u_e^2}{2h_e} g_2(\zeta) \tag{25}$$

where the normalized functions $g_1(\zeta)$ and $g_2(\zeta)$ are defined as

$$\left.\begin{aligned} g_1(\zeta) &\equiv F_1(\zeta)/F_1(\zeta_d) \\ g_2(\zeta) &\equiv F_2(\zeta) - g_1(\zeta)F_2(\zeta_d) \end{aligned}\right\} \tag{26}$$

in order to have the following boundary values

$$g_1(\zeta_d) = 1 \; ; \qquad g_1(\infty) = 0$$

$$g_2(\zeta_d) = 0 \; ; \qquad g_2(\infty) = 0$$

The functions $g_1(\zeta)$ and $g_2(\zeta)$ have been calculated from equations (23) and (26) using the numerical solution for $u_*(\zeta)$. These functions have been determined for Prandtl numbers of 0.1, 0.25, 0.5, 0.72, 1.0, 1.5, 2.0, and 10.0. Results are presented in table II. This table enables the enthalpy distribution to be calculated readily as a function of ζ. The Pr range of interest for gas flows is between about 0.25 and 1.0; the other values would correspond to liquids (when the density is constant

the present solution corresponds to the assumption of "constant properties").

For the special case of $Pr = 1$, equations (26) reduce merely to

$$(g_1)_{Pr=1} = 1 - u_* \qquad (g_2)_{Pr=1} = u_*(1 - u_*)$$

Equation (25) reduces to

$$(h_*)_{Pr=1} = 1 + \left(\frac{h_w}{h_e} - 1\right)(1 - u_*) + \frac{u_e^2}{2h_e} u_*(1 - u_*)$$

$$= \frac{h_w}{h_e} - u_*\left(\frac{h_w}{h_e} - 1 - \frac{u_e^2}{2h_e}\right) - u_*^2 \frac{u_e^2}{2h_e} \tag{27}$$

which is the well-known Crocco integral for viscous flow of a gas with Prandtl number of unity.

Velocity, Enthalpy, and Temperature Profiles in Physical Coordinates

As noted previously, the relation between ζ and y is determined by the equation

$$\frac{y}{2}\sqrt{\frac{u_e}{\nu_e x C}} = \int_0^\zeta T_* \frac{d\zeta}{2u_*} \tag{13}$$

This equation involves T_*, whereas the solution to the energy differential equation involves h_*. The $h(T)$ relationship for any gas obeying the equation of state $p = \rho RT$ is

$$h = c_{p_a} T + h_{int} \tag{28}$$

where $h_{int} \equiv \int_0^T c_{p_{int}} dT$ is the enthalpy for internal motion within the molecules, $c_{p_a} = \gamma_a R/(\gamma_a - 1)$ is the constant specific heat for the active degrees of freedom (translation and rotation), and $c_{p_{int}}$ is the temperature-dependent specific-heat contribution for the internal degrees of freedom (vibration and electronic excitation). A diatomic gas, or a gas with linear molecules, corresponds to $\gamma_a = 7/5$; a polyatomic gas corresponds to $\gamma_a = 4/3$. The total specific heat c_p is obtained by differentiating equation (28).

$$c_p = \frac{\gamma_a}{\gamma_a - 1} R + c_{p_{int}}$$

$$= \frac{\gamma_a}{\gamma_a - 1} R + \left(c_{p_{vib}} + c_{p_{elec}} \right) \tag{29}$$

For a given gas, h_{int} is a known function of T, which, in turn, is a known function of h. The $h_{int}(T)$ relationship is different for each gas having internal energy within a molecule. In terms of the function $(h_{int})_* \equiv h_{int}/h_e$ the dimensionless temperature can be expressed as

$$T_* \equiv \frac{T}{T_e} = \frac{h_e}{c_{p_a} T_e} \left(h_* - h_{*_{int}} \right) \tag{30}$$

which can be combined with equations (13) and (15) to yield

$$\frac{y}{2} \sqrt{\frac{u_e}{\nu_e x C}} = \frac{(\gamma_a - 1)}{\gamma_a} \frac{h_e}{R T_e} \left[\int_0^\zeta h_* \frac{d\zeta}{2u_*} - \int_0^\zeta (h_*)_{int} \frac{d\zeta}{2u_*} \right]$$

$$= \frac{(\gamma_a - 1) h_e}{\gamma_a R T_e} \left[\eta + \left(\frac{h_w}{h_e} - 1 \right) \eta_1 + \frac{u_e^2}{2h_e} \eta_2 - \int_0^\zeta (h_*)_{int} \frac{d\zeta}{2u_*} \right] \tag{31}$$

where the Prandtl number independent function $\eta(\zeta)$ is the same as previously defined by equation (15) (tabulated in table I), and the supplementary Prandtl number dependent functions $\eta_1(\zeta)$ and $\eta_2(\zeta)$ are defined by the equations

$$\left.\begin{aligned} \eta_1(\zeta) &\equiv \int_0^\zeta g_1(\zeta) \frac{d\zeta}{2u_*} \\ \eta_2(\zeta) &\equiv \int_0^\zeta g_2(\zeta) \frac{d\zeta}{2u_*} \end{aligned}\right\} \tag{32}$$

Values of η_1 and η_2 are tabulated in table III. Equation (31) enables the velocity and enthalpy profiles in ζ coordinates to be converted into the (x,y) physical coordinates. The enthalpy profiles together with the $h(T)$ function for a given gas enable the temperature profile to be determined. The velocity and temperature profiles, of course, determine the Mach number profiles.

For the special case of gases having a constant specific heat (which would be the case of gases having no vibration within molecules, or of gases over the special temperature range where the vibrational energy is fully excited) the equations relating y and ζ simplify considerably. The integral term in equation (31) vanishes since h_{int} is 0. Moreover, $h = [\gamma/(\gamma - 1)]RT$ for this special case. Consequently

$$\frac{y}{2}\sqrt{\frac{u_e}{\nu_e x C}} = \eta + \left(\frac{T_w}{T_e} - 1\right)\eta_1 + \frac{\gamma - 1}{2} M_e^2 \eta_2 \tag{33}$$

and the Mach number profile is determined by

$$M = M_e \frac{u_*}{\sqrt{T_*}} = \frac{M_e u_*}{\sqrt{1 + \left(\frac{T_w}{T_e} - 1\right)g_1 + \frac{\gamma - 1}{2} M_e^2 g_2}} \tag{34}$$

The total enthalpy profile

$$\frac{h_t}{h_{te}} = \frac{h_* + \frac{u_e^2}{2h_e} u_*^2}{1 + \frac{u_e^2}{2h_e}}$$

becomes for this special case

$$\frac{T_t}{T_{te}} = \frac{h_t}{h_{te}} = \frac{1 + \left(\frac{T_w}{T_e} - 1\right)g_1 + \frac{\gamma - 1}{2} M_e^2 (u_*^2 + g_2)}{1 + \frac{\gamma - 1}{2} M_e^2} \tag{35}$$

Heat Transfer and Recovery Factor at Wall

Inasmuch as the solution to the differential equations of viscous flow pertain to the motion only within the thin mixing layer, which is located a considerable distance from the wall surface, it is necessary to relate the rate of heat transfer at the wall to the properties of the mixing layer. This is done by means of the law of energy conservation.

Within any closed control surface A, the conservation of energy requires that

heat input across A	=	increase in internal energy and kinetic energy	+	work done by gas through normal pressures on A	+	work done by gas through tangential stresses on A

The work contribution of tangential stresses often is not considered in integral formulations of the energy conservation law, but it must be included here because of the type of contour selected subsequently. For steady flow, the energy law can be converted to the form

$$\iint_A \lambda \frac{\partial T}{\partial n} dA = \iint_A \left(e + \frac{V^2}{2}\right) \rho V_n dA + \iint_A p V_n dA + \iint_A \tau V_t dA \qquad (36)$$

where the various symbols are:

n coordinate normal to the surface A (positive if directed outward)

λ coefficient of heat conduction ($c_p \mu / Pr$)

e internal energy per unit mass ($h - p/\rho$)

V_n velocity component normal to A (positive if directed outward)

V_t velocity component tangential to A (positive if shear stress represents work done by gas within A)

τ shear stress tangential to A ($|\mu \partial u/\partial y|$)

Along a streamline V_n is 0, and along a wall V_t is 0; hence by applying this conservation theorem to the closed contour formed by the dividing streamline SR (designated by subscript o, as sketched in fig. 1) together with the wall boundary RS, there results

$$b \int_o^l \left(\lambda \frac{\partial T}{\partial y}\right)_o dx - Q_w = 0 + 0 + b \int_o^l \left(\mu \frac{\partial u}{\partial y}\right)_o (-u_o) dx \qquad (36a)$$

where b is the width of the two-dimensional flow, and where Q_w is the rate of heat addition to the wall ($-Q_w$ is the rate of heat addition to the gas). The tangential velocity u_o has a negative sign prefixed inasmuch as the shear stress τ does work on the gas. By solving

for Q_w, substituting $\lambda = c_p\mu/Pr$, and employing ζ as an independent variable, there results

$$\frac{Q_w}{b} = h_e \int_0^l \frac{\mu_o}{Pr}\left(\frac{dh_*}{d\zeta}\frac{\partial\zeta}{\partial y}\right)_o dx - u_e \int_0^l \mu_o\left(\frac{du_*}{d\zeta}\frac{\partial\zeta}{\partial y}\right)_o u_o dx \tag{37}$$

According to equation (22), $G(0) = 0$, hence differentiation of equation (21) yields

$$\left(\frac{dh_*}{d\zeta}\right)_o = - C_1 \frac{(4u_{*_o}u_{*_o}')^{Pr}}{2u_{*_o}} \tag{38}$$

Also, from equation (12)

$$\left(\frac{\partial\zeta}{\partial y}\right)_o = \frac{\rho_o u_o}{\rho_e\sqrt{\nu_e u_e x C}} \tag{39}$$

so that the integrals in equation (37) become $\left(\text{since } \rho_*\mu_* = C = \rho_{*_o}\mu_{*_o}\right)$

$$\frac{Q_w}{b} = h_e\sqrt{\rho_e u_e \mu_e l C}\left[-C_1 \frac{(4u_{*_o}u_{*_o}')^{Pr}}{Pr} + 2\frac{u_e^2}{h_e}u_{*_o}^2 u_{*_o}'\right] \tag{40}$$

This is a relatively simple equation inasmuch as u_{*_o} $(\equiv u_o/u_e)$ and u_{*_o}' $(\equiv du_*/d\zeta$ at $\zeta = 0)$ are constants independent of Pr, having the values 0.587 and 0.341, respectively.

Under adiabatic conditions at the wall $Q_w = 0$, and the value of the enthalpy at the wall is h_{aw}, so that by substituting C_1 from equation (24) into equation (40)

$$h_{aw_*} \equiv \frac{h_{aw}}{h_e} = 1 + \frac{u_e^2}{2h_e}\left[F_2(\zeta_d) + \frac{4Pru_{*_o}^2 u_{*_o}'}{(4u_{*_o}u_{*_o}')^{Pr}} F_1(\zeta_d)\right] \tag{41}$$

from which it is clear that the recovery factor r is as follows:

$$\frac{h_{aw} - h_e}{(u_e^2/2)} = \frac{h_{aw} - h_e}{h_t - h_e} \equiv r = F_2(\zeta_d) + \frac{4Pru_{*_o}^2 u_{*_o}'}{(4u_{*_o}u_{*_o}')^{Pr}} F_1(\zeta_d) \tag{42}$$

The dimensionless, average, heat-transfer rate per unit area $\bar{q}_w \equiv Q_w/bl$ becomes

$$\frac{\bar{q}_w}{\rho_e u_e (h_{aw} - h_w)} = \sqrt{\frac{C}{Re}} \frac{(4u_{*_o} u_{*_o}')^{Pr}}{PrF_1(\zeta_d)} \tag{43}$$

Numerical computations of r from equation (42) are tabulated in column (a) of table IV. Values of $\bar{q}_w \frac{\sqrt{Re/C}}{\rho_e u_e (h_{aw} - h_w)}$ computed from equation (43) are tabulated in column (c) of table IV.

Heat Transfer When Gas Is Injected Into Separated Region

It is surprisingly easy to generalize the preceding analysis in order to consider conditions where gas is injected into the dead-air region. When a mass flow m_i is injected, there no longer is an equality between the mass flux drawn out along the mixing layer and the mass flux reversed near the reattachment zone. Instead, in a steady flow, the same amount of mass flow m_i as is injected into the dead-air region also would pass downstream near reattachment between the dividing streamline and some streamline displaced at a distance y_i below the dividing streamline.

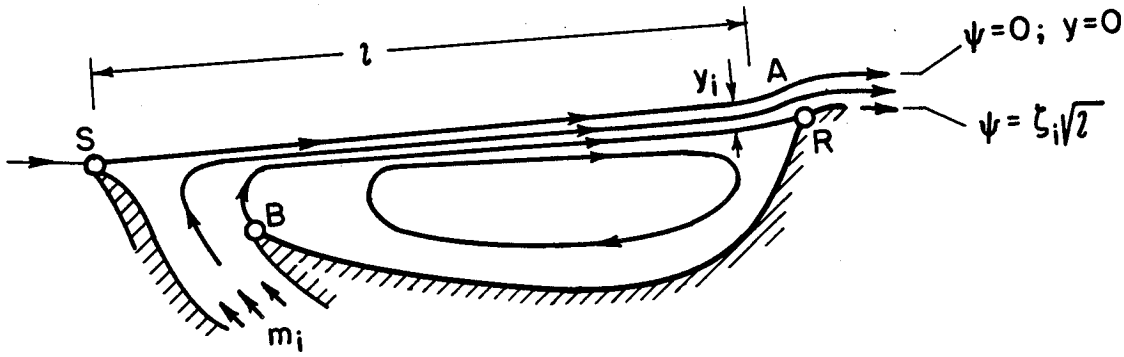

As indicated in the sketch, where only those streamlines below the dividing streamline are drawn, the mass-flow parameter corresponding to the particular streamline displaced a distance y_i from the dividing streamline is designated as ζ_i. The equation for the balance between mass flow injected (near B) and mass flow escaping (near R) is

$$\frac{m_i}{b} = \int_{y_i}^{0} \rho u \, dy = \sqrt{\rho_e u_e \mu_e l C} \int_{\zeta_i}^{0} d\zeta = -\zeta_i \sqrt{\rho_e u_e \mu_e l C} \tag{44}$$

The law of conservation of energy for the contour RBSAR in the sketch is (see eq. (36))

$$b\int_0^l \left(\lambda \frac{\partial T}{\partial y}\right)_0 dx - Q_w = h_i m_i + b\int_y^0 \left(h + \frac{u^2}{2}\right)\rho u\, dy + b\int_0^l \left(\mu \frac{\partial u}{\partial y}\right)_0 (-u_0)dx$$

which becomes, after dimensionless variables are introduced and the assumption is made that the enthalpy of the injected gas (h_i) is a constant equal to the enthalpy at the wall,

$$\frac{Q_w}{h_e\sqrt{\rho_e u_e \mu_e l C}} = b\int_{\zeta_d}^{\zeta_i} \left(h_* - h_{w_*} + \frac{u_e^2}{2h_e} u_*^2\right)d\zeta \tag{45}$$

This equation perhaps could have been written down directly by considering the conservation of energy for a contour comprising the streamline BR and the wall RB. It also can be expressed in terms of $\bar{q}_w \equiv Q_w/bl$ as

$$\frac{\bar{q}_w l}{h_e\sqrt{\rho_e u_e \mu_e l C}} = \int_{\zeta_d}^{\zeta_i} \left(h_* - h_{w_*} + \frac{u_e^2}{2h_e} u_*^2\right)d\zeta \tag{46}$$

or, by using equations (21), (23), and (24)

$$\frac{\bar{q}_w l}{h_e\sqrt{\rho_e u_e \mu_e l C}} = -C_1 F_1(\zeta_d) I_1(\zeta_i) + \frac{u_e^2}{2h_e} I_2(\zeta_i) \tag{47}$$

where the functions I_1 and I_2 are defined as

$$I_1(\zeta) \equiv \int_{\zeta_d}^{\zeta} \left[1 - \frac{F_1(\zeta)}{F_1(\zeta_d)}\right]d\zeta \equiv \int_{\zeta_d}^{\zeta} [1 - g_1(\zeta)]d\zeta \tag{48}$$

$$I_2(\zeta) \equiv \int_{\zeta_d}^{\zeta} [F_2(\zeta) - F_2(\zeta_d) + u_*^2]d\zeta \equiv -I_1(\zeta)F_2(\zeta_d) + \int_{\zeta_d}^{\zeta} [g_2(\zeta) + u_*^2]d\zeta \tag{49}$$

By substituting into equation (46) the expression for C_1 from equation (24) and dividing by the rate of heat transfer without injection, there results

$$\frac{Q_w}{(Q_w)_{\zeta_i=0}} = \frac{\bar{q}_w}{(\bar{q}_w)_{\zeta_i=0}} = \frac{\frac{u_e^2}{2h_e}\left[F_2(\zeta_d)I_1(\zeta_i) + I_2(\zeta_i)\right] - \left(\frac{h_w}{h_e} - 1\right)I_1(\zeta_i)}{\frac{u_e^2}{2h_e}\left[F_2(\zeta_d)I_1(0) + I_2(0)\right] - \left(\frac{h_w}{h_e} - 1\right)I_1(0)} \tag{50}$$

The value for the recovery factor is

$$r = F_2(\zeta_d) + \frac{I_2(\zeta_i)}{I_1(\zeta_i)} \tag{51}$$

These equations depend only on the mass flow injected into the dead-air region, as determined by the dimensionless variable ζ_i. The calculation of the recovery factor and heat transfer in a given case requires a knowledge of the functions I_1 and I_2 which are tabulated in table V, and the constant $F_2(\zeta_d)$ which depends only on the Prandtl number as tabulated earlier.

Skin Friction

By applying the momentum conservation law to the same closed contour as that to which the energy conservation law was applied (contour composed of dividing streamline SR in fig. 1 together with wall boundary RS), the effective skin friction can be estimated. Inasmuch as there is no mass flux in or out of this contour, momentum conservation requires that

$$\begin{matrix}\text{force on wall} \\ \text{in x direction}\end{matrix} \equiv F_x = b\int_0^{x_R}\left[\left(\mu\frac{\partial u}{\partial y}\right)_0 + (p_e - p)\cos(n,x)\right]dx \tag{52}$$

where (n,x) is the angle between the x direction and the outward normal direction, and x_R is the distance to the reattachment point. It is seen that the term involving pressure does not vanish as it did in the energy conservation integral. This is because p in the momentum integral is multiplied by the nonzero term $\cos(n,x)$, whereas p in the energy integral is multiplied by the normal velocity component V_n which vanishes for the particular contour selected. The term involving $\cos(n,x)$ depends on the exact shape of streamlines near reattachment, and would be different for each flow. Consequently, it does not seem possible to make any more than a rough estimate of the skin friction for the general case. Such an estimate can be made by disregarding the term $(p_e - p)\cos(n,x)$

which is zero everywhere except near the reattachment zone (where locally p departs from p_e). Thus,

$$C_F \equiv \frac{F_x}{\frac{1}{2}\rho_e u_e^2 (bl)} \sim \frac{2}{\rho_e u_e^2 l} \int_0^l \left(\mu \frac{\partial u}{\partial y}\right)_0 dx \tag{53}$$

By using equation (39) and noting that $(\rho_* u_*)_0 = C$, the integral becomes

$$C_F \sim 4 u_{*_0} u_{*_0}' \sqrt{\frac{C}{Re}} = 0.80 \sqrt{\frac{C}{Re}} \tag{54}$$

It will be seen shortly that this estimate of skin friction is the same as that which would be obtained by arbitrarily applying Reynolds analogy to the heat-transfer rate calculated for Pr = 1.

If gas is injected into the dead-air region either at low velocity or in the direction normal to the mixing layer, then only one additional term

$$-b \int_{y_i}^{0} \rho u^2 dy$$

must be added to equation (52) for skin friction. Conservation of momentum within the portion of mixing layer below the dividing streamline, however, requires that

$$\int_0^l \left(\mu \frac{\partial u}{\partial y}\right)_0 dx = \int_{-\infty}^{0} \rho u^2 dy$$

From equation (12) it is seen that

$$\int \rho u^2 dy = u_e \rho_e \sqrt{\nu_e u_e l C} \int u_* d\zeta \tag{55}$$

so that the estimate of skin friction with injection can be written as

$$C_F \sim 2\sqrt{\frac{C}{Re}} \left(\int_{\zeta_d}^{0} u_* d\zeta - \int_{\zeta_i}^{0} u_* d\zeta \right) = 2\sqrt{\frac{C}{Re}} \int_{\zeta_d}^{\zeta_i} u_* d\zeta \tag{56}$$

For the special case of no injection, integration of the $u_*(\zeta)$ function (table I) yields

$$(C_F)_{\zeta_i=0} \sim 0.796\sqrt{\frac{C}{Re}}$$

in agreement with equation (54).

RESULTS AND DISCUSSION

Comparison With Results for Laminar Boundary Layers

Recovery factor.- A good way to visualize the results of the preceding analysis is to compare them with corresponding calculations for a flat plate over which a constant-pressure laminar boundary layer flows. The two functions g_1 and g_2, which combine linearly to yield the enthalpy-velocity relationship for a separated laminar mixing layer (according to eq. (25)) are shown in figure 2. Also shown for purposes of comparison are the corresponding two functions for a laminar boundary layer (according to the analysis of refs. 5 and 8). For $Pr = 1$ the g_1 and g_2 functions are equal to $1 - u_*$ and $u_*(1 - u_*)$, respectively; these quantities also are shown in figure 2. As might have been anticipated for Pr near 1, the component functions for enthalpy are much the same for the two types of viscous layer. Since the recovery factor is merely a measure of the enthalpy when the velocity is zero, it too should be nearly the same for the two types of laminar flow. The recovery factor for a flat plate in an incompressible stream is very nearly equal to $\sqrt{Pr}$, as first calculated by Pohlhausen (ref. 9). In a compressible stream the recovery factor is unaffected by variation of Mach number within the framework of assumptions made in the present analysis. A comparison of $\sqrt{Pr}$ with the values of recovery factor computed herein for separated laminar flows is made in the following table:

Recovery factor in separated flow		$\sqrt{Pr}$
Pr	r	
0.1	0.361	0.316
.25	.504	.500
.5	.712	.707
.72	.850	.849
1.0	1.000	1.000
1.5	1.228	1.225
2.0	1.423	1.414
10.0	3.27	3.16

It is seen that the recovery factor for pure laminar separated regions is approximately equal to $\sqrt{Pr}$. Consequently the recovery factors for a separated mixing layer and an attached boundary layer are essentially the same.

Rate of heat transfer.- A comparison of the corresponding rates of heat transfer yields different results. For the flow of a compressible laminar boundary layer over a flat plate under the same framework of assumptions as employed herein, the average rate of heat transfer $(\bar{q}_w)_{bl}$ according to references 5 and 8 is

$$\frac{(\bar{q}_w)_{bl}}{\rho_e u_e (h_w - h_{aw})}\sqrt{\frac{Re}{C}} = \frac{Y_o'(0)}{Pr} \quad \left(\approx 0.664\,Pr^{-2/3} \text{ for } Pr \text{ near } 1\right) \qquad (57)$$

A comparison with the rate of heat transfer for the pure laminar type of separated flow is made in the following table:

Separated mixing layer		Boundary layer	$\frac{\bar{q}_w}{(\bar{q}_w)_{bl}}$
Pr	$\frac{\bar{q}_w\sqrt{Re/C}}{\rho_e u_e (h_w - h_{aw})}$	$\frac{(\bar{q}_w)_{bl}\sqrt{Re/C}}{\rho_e u_e (h_w - h_{aw})}$	
0.1	0.833	2.70[a]	0.31
.25	.674	1.57[a]	.43
.5	.526	1.03	.51
.72	.457	.820	.56
1.0	.399	.664	.60
1.5	.335	.510	.66
2.0	.293	.421	.70
10.0	.135	.146	.92

[a]The calculations of boundary-layer flow for small Prandtl numbers (e.g., for Pr = 0.1 and 0.25) are based primarily on appropriate small Pr expansion formulae developed by P. Lagerstrom and H. Liepmann in some unpublished research.

In calculating the ratio $\bar{q}_w/(\bar{q}_w)_{bl}$ it is assumed that the values of ρ_e, u_e, Re, and h_w/h_e are the same for the two cases. It is to be noted that the ratio $\bar{q}_w/(\bar{q}_w)_{bl}$ of the two heat fluxes is independent of M_e, Re, and h_w/h_e. For air (Pr ≈ 0.72), the calculated heat transfer in a separated laminar mixing layer is 0.56 of that for a corresponding attached laminar boundary layer.

Attention is called to the fact that the use of the integral form of the energy conservation law enabled only the average (or over-all) rate of heat transfer $\bar{q}_w$ to be calculated and not the local rate. In this respect, the present analysis of separated flows is unlike the analysis of an attached laminar boundary layer wherein both the local distribution and the average rate of heat transfer can be calculated. The local distribution of heat flux along the wall of a separated flow would depend on the details of the vortex-like motion within the region of dead air lying between the wall and the thin mixing layer. Without considering these details together with the particular shape of the wall, the theory cannot provide information about the local rate of heat transfer.

Skin friction.- Since $(C_F)_{bl}$ for an attached laminar boundary layer is $1.328\sqrt{C/Re}$ (see ref. 5), it follows from equation (54) that the estimated value for effective friction of a separated laminar mixing layer is $0.80/1.328 = 0.60$ of that for the corresponding attached laminar boundary layer. At $Pr = 1$ the heat flux, as tabulated above, also is 0.60 of that for the corresponding attached laminar boundary. Thus the estimate of skin friction is the same as that which would be obtained by arbitrarily applying Reynolds analogy.

Velocity and temperature profiles.- To illustrate further the relative characteristics of separated layers and attached boundary layers, a comparison of both types of layer for $M_e = 10$ is presented in figures 3 and 4 showing velocity and temperature profiles, respectively. The two extreme conditions of $T_w/T_e = 1$ and $T_w = T_{aw}$ are considered, as well as a third condition representing $T_w/T_e = 4$. These examples illustrate both some differences and similarities between a separated mixing layer and an attached boundary layer. For example, mixing layers are several times thicker than boundary layers, yet the maximum temperature attained within each layer for cold-wall conditions is essentially the same.

Flow with gas injection.- Numerical results illustrating the effect of mass injection on recovery factor in separated flow are presented in figure 5 for the values $Pr = 0.5$, 0.72, and 1.0. It is evident that for $Pr = 1$ the recovery factor is unaffected by mass injection and is the same for the separated mixing layer as it is for the attached laminar layer. When $Pr < 1$, however, the recovery factor is lowered substantially by injection, for both mixing layer and boundary layer. The curve representing the laminar boundary layer with mass injection (dotted line in fig. 5) is taken from the calculations of Low (ref. 10) which are based on the same viscosity-temperature relationship as is used herein.

The effect of gas injection on heat-transfer rate can be conveniently illustrated through consideration of several special cases which simplify the general equation (50). First, for the special case of $h_w/h_e = 1$

(which would imply $T_w/T_e = 1$ if the specific heat were constant), then equation (50) becomes

$$\left[\frac{Q_w}{(Q_w)_{\zeta_i=0}}\right]_{h_w=h_e} = \frac{F_2(\zeta_d)I_1(\zeta_i) + I_2(\zeta_i)}{F_2(\zeta_d)I_1(0) + I_2(0)} \tag{58a}$$

which is independent of Mach number. Also, if the Mach number is very large so that $M_e^2 >> (h_w/h_e - 1)$ (or $u_e^2/2h_e >> (h_w/h_e - 1)$), then equation (50) again reduces to the same expression

$$\left[\frac{Q_w}{(Q_w)_{\zeta_i=0}}\right]_{M_e=\infty} = \frac{F_2(\zeta_d)I_1(\zeta_i) + I_2(\zeta_i)}{F_2(\zeta_d)I_1(0) + I_2(0)} \tag{58b}$$

For gases, expressions (58) also are nearly independent of the Prandtl number, as the curves in figure 6 illustrate for $Pr = 0.5$, 0.72, and 1.0. If a different limiting case is considered, namely, $M_e \to 0$, then $u_e^2/2h_e << (h_w/h_e - 1)$, and equation (50) becomes

$$\left[\frac{Q_w}{(Q_w)_{\zeta_i=0}}\right]_{M_e=0} = \frac{I_1(\zeta_i)}{I_1(0)} \tag{59}$$

Numerical calculations show this ratio to be only slightly higher than the ratio given by equation (58). For example, at $-\zeta_i = 0.4$, the ratio in equation (58) representing $M_e \to \infty$, or $h_w = h_e$, is 0.49 (for $Pr = 0.72$), whereas the ratio in equation (59) representing $M_e \to 0$ is 0.52. For practical purposes, then, the curves in figure 6 are applicable to a wide variety of conditions.

As perhaps might be anticipated, the effect of mass injection on the estimated skin friction is much the same as the effect on heat transfer. At $Pr = 1$, for example, g_1 is equal to $1 - u_*$, as previously noted, so the combination of equations (48) and (56) yields for the ratio of estimated skin friction with injection to that without injection

$$\left[\frac{C_F}{(C_F)_{\zeta_i=0}}\right]_{Pr=1} = \frac{I_1(\zeta_i)}{I_1(0)} \tag{60}$$

This ratio is identical to the corresponding ratio of heat-transfer rates, as indicated by equation (59) for low-speed flow. Inasmuch as the ratio

in equation (59) is practically the same as that in equations (58), it follows that the effect of mass injection on estimated skin friction is - for practical purposes - essentially the same as the effect on heat-transfer rate (as represented by the curves in figure 6).

Computational Checks and Extensions of Analysis

It was found possible to obtain an independent check on the internal consistency of the numerical calculations by employing certain integral considerations other than those used in the main analysis. An example of such a check already has been observed. The quantity $C_F\sqrt{Re/C}$ for separated flow without injection is equal to the differential expression $4u_{*_O}u_{*_O}'$, according to equation (54), yet also should be equal to the integral expression $2\int_{\zeta_d}^{\zeta_O} u_* d\zeta$, according to equation (56). The table of $u_*(\zeta)$ yields values of 0.801 and 0.796, respectively, for these two independent expressions. This is considered to be adequate agreement for present purposes. Similarly, independent integral checks (usually to within a few-tenths of 1 percent) of the differential expressions for both recovery factor and heat-transfer rate were obtained for all Prandtl numbers. Details are presented in Appendix A.

Probably the most significant feature of the integral method employed to check computations is that it yields equations which also can be applied to turbulent separated flows, provided the velocity profiles in the turbulent mixing layer are known. Details of the application to turbulent separation are presented in Appendix B. It will suffice here to note that velocity-profile data for turbulent mixing layers at high Mach numbers are not yet available, so the numerical calculations are restricted to low Mach numbers where such data are available. The calculated results for low-speed flow indicate that the heat-transfer rate to a separated turbulent flow is much higher than that to a comparable attached turbulent boundary layer. This result for turbulent flows contrasts sharply with the corresponding result for laminar flows.

Two other extensions can be made to the analysis. One is to axially symmetric flow, which is a rather simple extension and is presented in Appendix C. The other is to separated flows wherein the boundary-layer thickness at separation δ_s is sizable. This is not a simple extension. Equation (36a) would apply directly to this more general case, but great difficulty would be encountered in computing $(\partial T/\partial y)_O$, $(\partial u/\partial y)_O$, and u_O at various stations along the dividing streamline of the mixing layer. In effect, the absence of similar profiles for the case where δ_s is not zero would require that partial differential equations be solved for $u(x,y)$ and $T(x,y)$, rather than ordinary differential equations.

Some Practical Aspects of Gas Injection

The practical aspects of gas injection for separated flows are expected to be quite different than for flows of an attached laminar boundary layer. It is well known that the injection of gas through a porous wall unfortunately has a strong destabilizing effect on the laminar boundary-layer flow along that wall. There is no evident reason, however, to expect that the gas injection into a separated region through a porous wall, which is displaced a considerable distance from the separated laminar mixing layer, would necessarily have a strong destabilizing effect on the stability of the mixing layer. Such injection, if properly done, might have a favorable effect on stability inasmuch as the pressure rise near reattachment is reduced when gas is injected, and this pressure rise is important to the stability of the laminar flow. Some experiments on the effect of injection on stability clearly are in order.

If a mass flux of gas equal in magnitude to

$$\int_{-\infty}^{0} \rho u \, dy = \sqrt{\rho_e u_e \mu_e l C} \int_{\zeta_d}^{0} d\zeta = -\zeta_d \sqrt{\rho_e u_e \mu_e l C} \tag{65}$$

is injected into a separated region, then no air would be reversed near the reattachment zone. For this particular quantity of injection the heat transfer (and the estimated skin friction) would be zero. In mathematical terms, for $\zeta_i = \zeta_d$, then $I_1(\zeta_d) = I_2(\zeta_d) = 0$ and Q_w is therefore zero (see eq. (50)). It is interesting to consider an example in order to obtain a physical feeling for the magnitude which this particular rate of mass injection would represent in a practical case. Consider first, as sketched, a cone with 30° total included angle, a base radius

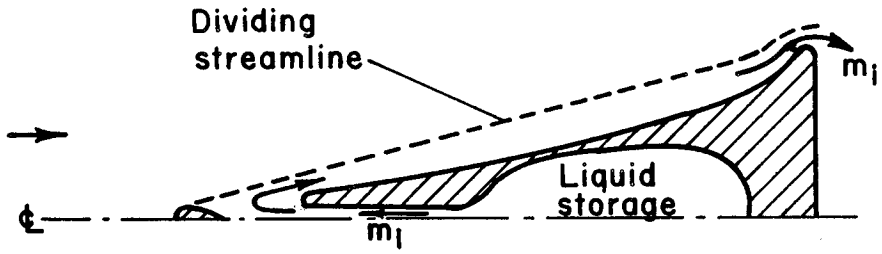

of 1 foot, flying at a Mach number of 20 at an altitude of 100,000 feet, and containing initially 1/3 of its volume as stored liquid air (or liquid nitrogen). For the case $\zeta_i = \zeta_d$, for which $Q_w = 0$, the cone would travel in steady flight a distance of approximately 1.4×10^6 body diameters (or about 500 miles) before the stored liquid had been completely injected into the separated region. Along this length of flight path, the heat transfer would be zero. After all mass had been expended, the rate of heat transfer would be 0.56 of that for a cone of 15° semiangle (provided the separated layer remained laminar).

Inasmuch as the quantities of mass injection required are relatively low, the scheme of mass injection into separated regions may have practical application. The degree of practicality depends upon the Reynolds numbers up to which separated mixing layers can be maintained laminar. Experiments are required to ascertain this under the conditions of hypersonic flight where the wall is cool compared to stagnation conditions and where gas is injected into the separated region.

CONCLUSIONS

The conclusions which follow have been obtained from an analysis of separated laminar flows wherein the thickness of the boundary layer is zero at the separation point:

1. The recovery factor in regions of separated laminar flow is approximately equal to the square root of the Prandtl number (to within 1 percent over the range of Prandtl numbers between 0.25 and 2.0) and, hence, is essentially the same as that of an attached laminar boundary-layer flow.

2. The calculated rate of heat transfer from a separated laminar mixing layer is less than that from an attached laminar boundary layer at corresponding values of Mach number, Reynolds number, and wall to stream temperature ratio; the ratio of the heat flux in the separated flow to that in the attached flow is a function only of the Prandtl number, and has the numerical value of 0.56 for $Pr = 0.72$ (the value for air).

3. Injection of gas into the dead-air region of a separated laminar flow is calculated to have a powerful effect in reducing heat-transfer rates, inasmuch as a moderate quantity of injection can reduce the heat flux to zero.

4. The effective skin friction for separated laminar flows is estimated to be about 0.6 of that for an attached laminar boundary-layer flow, and is affected by gas injection in essentially the same way as heat transfer is.

Ames Aeronautical Laboratory
National Advisory Committee for Aeronautics
Moffett Field, Calif., June 25, 1956

APPENDIX A

CONTOUR INTEGRAL CHECKS ON ACCURACY OF NUMERICAL CALCULATIONS

A check for internal consistency on the numerical calculation of $u_*(\zeta)$ can be obtained by noting that the conservation law of linear momentum in the x direction, when applied to a contour enclosing the mixing layer, requires that

$$\int_{-\infty}^{0} \rho u^2 dy = \int_{0}^{\infty} \rho u(u_e - u)dy$$

In (x,ζ) coordinate system, this requirement becomes

$$\int_{\zeta_d}^{0} u_* d\zeta = \int_{0}^{\infty} (1 - u_*)d\zeta \tag{A1}$$

Numerical evaluation of these two integrals from the $u_*(\zeta)$ solution yields

$$\int_{\zeta_d}^{0} u_* d\zeta = 0.398 \tag{A2}$$

and

$$\int_{0}^{\infty} (1 - u_*)d\zeta = 0.399 \tag{A3}$$

These two integrals agree within 0.25 percent. As a further check on u_*, it may be noted from the differential equation (11) that when $u_* = 0$, $(du_*/d\zeta)_{\zeta_d}$ must be the same as $-\zeta_d/2$. The values in table I show that $(du_*/d\zeta)_{\zeta_d} = +0.620$ and $-\zeta_d/2 = +0.617$. These values check within 0.5 percent.

Checks on the calculations of r and Q_w can be obtained from the energy conservation law by considering a contour enclosing only the dead-air region. The flux of energy fed into the dead-air region near the reattachment zone is

$$b\int_{-\infty}^{0} \left(h + \frac{u^2}{2}\right)\rho u \, dy$$

This energy flux is transported by the mass flux $b\int_{-\infty}^{0} \rho u\, dy$, which must be equal to the mass flux reversed by the pressure rise near the reattachment zone. (This mass flux, in turn, must also be equal to the mass flux re-entering the mixing layer after some heat energy has been imparted to the wall.) When this mass flux leaves the dead-air region and enters the mixing layer, it transports an energy flux of

$$b\int_{0}^{l} h_w \rho_w v_w dx$$

which, from the continuity equation, is equal to

$$b\int_{-\infty}^{0} h_w \rho u\, dy$$

Consequently, the rate of heat transfer to the wall must be the difference between these two energy fluxes.

$$Q_w = b\int_{-\infty}^{0} \left(h - h_w + \frac{u^2}{2}\right)\rho u\, dy \tag{A4}$$

In dimensionless variables,

$$Q_w = bh_e\sqrt{\rho_e u_e \mu_e l C}\int_{\zeta_d}^{0} \left(h_* - h_{w*} + \frac{u^2}{2h_e}\right) d\zeta \tag{A5}$$

By substituting h_* from equation (21), and setting $Q_w/bl = \bar{q}_w$, there is obtained

$$\frac{\bar{q}_w}{\rho_e u_e h_e}\sqrt{\frac{Re}{C}} = C_1\int_{\zeta_d}^{0} [F_1(\zeta) - F_1(\zeta_d)]\, d\zeta + \frac{u_e^2}{2h_e}\int_{\zeta_d}^{0} [F_2(\zeta) - F_2(\zeta_d)]\, d\zeta +$$

$$\frac{u_e^2}{2h_e}\int_{\zeta_d}^{0} u_*^2 d\zeta \tag{A6}$$

Under adiabatic wall conditions $\bar{q}_w = 0$, and $h_w = h_{aw}$; hence by substituting C_1 from equation (24)

$$\frac{h_{aw}}{h_e} = 1 + \frac{u_e^2}{2h_e}\left\{F_2(\zeta_d) - F_1(\zeta_d)\frac{\int_{\zeta_d}^{0}[F_2(\zeta) - F_2(\zeta_d) + u_*^2]d\zeta}{\int_{\zeta_d}^{0}[F_1(\zeta) - F_1(\zeta_d)]d\zeta}\right\}$$

from which it follows that an expression alternate to equation (42) for the recovery factor is

$$r = F_2(\zeta_d) - F_1(\zeta_d)\frac{\int_{\zeta_d}^{0}[F_2(\zeta) - F_2(\zeta_d) + u_*^2]d\zeta}{\int_{\zeta_d}^{0}[F_1(\zeta) - F_1(\zeta_d)d\zeta} = F_2(\zeta_d) + \frac{I_2(0)}{I_1(0)} \qquad (A7)$$

where the functions I_2 and I_1 are, as defined previously by equations (48) and (49)

$$I_1(\zeta) \equiv \int_{\zeta_d}^{\zeta}[1 - g_1(\zeta)]d\zeta$$

$$I_2(\zeta) \equiv \int_{\zeta_d}^{\zeta}[F_2(\zeta) - F_2(\zeta_d) + u_*^2]d\zeta$$

Expression (A7) should be numerically equal to the different expression of equation (42). The corresponding alternate expression for the rate of heat transfer is

$$\frac{\bar{q}_w}{\rho_e u_e(h_{aw} - h_w)} = \sqrt{\frac{C}{Re}}\int_{\zeta_d}^{0}[1 - g_1(\zeta)]d\zeta \qquad (A8)$$

which should be equal to the expression of equation (43).

Values of r computed from the alternate equation (A7) are tabulated in column (b) of table IV. Compared with the values in column (a) originally computed from equation (42), it is seen that the alternate independent calculations agree rather well with the original computations. The largest discrepancy amounts to 0.2 percent for values of Prandtl number less than 2. For a Prandtl number of 10, the two computations differ by 3 percent. In this latter case, the values from the integral method (eq. (A7)) are regarded as less accurate, inasmuch as their evaluation

involved several quadratures of functions such as u_*^{Pr} which, for Pr = 10, vary so rapidly that high accuracy could not be obtained with the intervals selected. Nevertheless, the over-all agreement between the two independent methods of computation is regarded as satisfactory. Similarly, a satisfactory check on numerical computations of $\bar{q}_w$ by the two independent methods is obtained, as evidenced by comparison of columns (c) and (d) in table IV. Compared with the original calculations from equation (43) (column (c)), the calculations from the alternate equation (A8) (column (d)), agree to within 0.5 percent for all values of Prandtl number.

APPENDIX B

HEAT TRANSFER IN SEPARATED TURBULENT FLOWS

Although complete calculations cannot at present be made for separated, compressible, turbulent mixing layers, certain of the ideas developed nevertheless can be applied to such cases. For this purpose it is assumed that the Prandtl number is unity. Equation (A4) was developed from general energy considerations and is applicable also to turbulent flows.

$$Q_w = b\int_{-\infty}^{0}\left(h - h_w + \frac{u^2}{2}\right)\rho u\, dy \tag{B1}$$

The assumption Pr = 1 enables the relation between enthalpy and velocity to be expressed as the Crocco integral,

$$h_* = 1 + \left(\frac{h_w}{h_e} - 1\right)(1 - u_*) + \frac{u_e^2}{2h_e}u_*(1 - u_*)$$

$$= \frac{h_w}{h_e} + u_*\left(1 + \frac{u_e^2}{2h_e} - h_{w_*}\right) - u_*^2\frac{u_e^2}{2h_e} \tag{B2}$$

so that the average rate of heat transfer becomes, after some algebraic manipulation wherein the relationship $h_{aw_*} = (u_e^2/2h_e) + 1$ is used and the dimensionless variable $\xi \equiv \sigma y/x$ is introduced,

$$\frac{\bar{q}_w}{\rho_e u_e(h_{aw} - h_w)} = \frac{1}{\sigma}\int_{-\infty}^{0}\rho_* u_*^2 d\xi = \frac{1}{\sigma h_{w_*}}\int_{-\infty}^{0}\frac{u_*^2 d\xi}{1 + u_*\left(\frac{h_{aw}}{h_w} - 1\right) - u_*^2\frac{u_e^2}{2h_w}} \tag{B3}$$

where the constant σ is inversely proportional to the rate of spread of the turbulent mixing layer. Clearly, it is necessary to know the velocity distribution $u_*(\xi)$ within a turbulent mixing layer, and the rate of spread σ, before the average rate of heat transfer can be calculated. Such knowledge, unfortunately, is not yet available except for two cases.

For the limiting case of zero Mach number, the velocity distribution and rate of spread are known from the paper of Tollmien (ref. 11). By

substituting Tollmien's velocity distribution ($\sigma = 12$ at $Re = 2.5 \times 10^6$ from his experiments) into equation (B3) there results

$$\frac{\bar{q}_w}{\rho_e u_e (h_{aw} - h_w)} = 0.012$$

which leads to an interesting result when comparison is made to a corresponding attached turbulent boundary layer. At the same Reynolds number as in Tollmien's experiments, the corresponding heat-transfer parameter for a turbulent boundary layer of constant pressure would be approximately

$$\left[\frac{\bar{q}_w}{\rho_e u_e (h_{aw} - h_w)}\right]_{bl} = (St)_{bl} = \frac{C_F}{2} = 0.0019$$

which indicates the heat transfer in separated turbulent flow not to be smaller than in a turbulent boundary layer, but to be, in fact, $\frac{0.012}{0.0019} = 6.3$ times as large. This comparison is in sharp contradistinction to the analogous comparison for the laminar case where the corresponding ratio is about 0.6 rather than 6.3.

It is to be noted that the data available at present for compressible turbulent mixing layers indicate the Mach number to have a pronounced effect on the integral in equation (B3). The data of Gooderum, Wood, and Brevoort (ref. 12) at a Mach number of 1.6 indicate that the rate of spread (about 9° angle) of turbulent mixing layer is much less than at low speed (about 14° angle); hence the integral in equation (B3) also would be proportionately less. Consideration also of the density change on going from $M = 0$ to $M = 1.6$ would then yield a value for this integral 57 percent less than that at low speed, which is equivalent to a heat flux in turbulent separated flow of about 2.8 times that in a corresponding turbulent boundary layer. The ratio of heat fluxes, amounting to 6.3 at $M_e = 0$, and 2.8 at $M_e = 1.6$, obviously is strongly dependent on Mach number. Consequently, if the marked trend persists, a separated turbulent flow might not have a greater heat flux than a turbulent boundary-layer flow at sufficiently high Mach numbers. Experiments on the rate of spread and on the velocity distribution within turbulent mixing layers at high supersonic speeds are required before this can be ascertained.

APPENDIX C

APPLICATION TO AXIALLY SYMMETRIC FLOW

Although the analysis as developed applies directly to two-dimensional flow only, it can be easily extended to axially symmetric flow by employing Mangler's transformation. This transformation for a constant-pressure, separated, laminar mixing layer is identical to that for a laminar boundary layer. For a given Reynolds number and Mach number, the mixing-layer thickness in axially symmetric flow is $1/\sqrt{3}$ times that in two-dimensional flow. Consequently, the heat-transfer rate, in place of equation (45), is given by the equation

$$\frac{Q_w}{h_e\sqrt{\rho_e u_e \mu_e l C}} = \frac{2\pi r_b}{\sqrt{3}} \int_{\zeta_d}^{\zeta_i} \left(h_* - h_{w_*} + \frac{u_e^2}{2h_e} u_*^2 \right) d\zeta \tag{C1}$$

and hence the average heat-transfer rate per unit area $\bar{q}_w \equiv Q_w/\pi r_b l$ is

$$\frac{\bar{q}_w l}{h_e\sqrt{\rho_e u_e \mu_e l C}} = \frac{2}{\sqrt{3}} \int_{\zeta_d}^{\zeta_i} \left(h_* - h_{w_*} + \frac{u_e^2}{2h_e} u_*^2 \right) d\zeta \tag{C2}$$

which is seen, by comparison with equation (46) to be $2/\sqrt{3}$ times as large as for two-dimensional flow, just as it is in the case of comparison of an attached boundary layer on a cone with the corresponding laminar boundary layer on a plate. Consequently, the ratio $\bar{q}_w/(\bar{q}_w)_{bl}$ tabulated previously for two-dimensional flow also applies directly to axially symmetric flow. If gas is injected into an axially symmetric region of separated flow, then for the same fractional reduction in heat-transfer rate (same value of $\bar{q}_w/(\bar{q}_w)_{\zeta_i=0}$) the value of $-\zeta_i = \dfrac{(2/\sqrt{3})(m_i/\pi r_b l)}{\sqrt{\rho_e u_e \mu_e C/l}}$ in the axially symmetric flow would be the same as the value of $\dfrac{m_i/bl}{\sqrt{\rho_e u_e \mu_e C/l}}$ in the two-dimensional flow.

REFERENCES

1. von Doenhoff, Albert E.: A Preliminary Investigation of Boundary-Layer Transition Along a Flat Plate with Adverse Pressure Gradient. NACA TN 639, 1938.

2. Chapman, Dean R., Kuehn, Donald M., and Larson, Howard K.: Preliminary Report on a Study of Separated Flows in Supersonic and Subsonic Streams. NACA RM A55L14, 1956.

3. Stalder, Jackson R., and Nielsen, Helmer V.: Heat Transfer From a Hemisphere-Cylinder Equipped With Flow Separation Spikes. NACA TN 3287, 1954.

4. Chapman, Dean R.: Laminar Mixing of a Compressible Fluid. NACA Rep. 958, 1950.

5. Chapman, Dean R., and Rubesin, Morris W.: Temperature and Velocity Profiles in the Compressible Laminar Boundary Layer with Arbitrary Distribution of Surface Temperature. Jour. Aero. Sci., vol. XVI, no. 9, Sept. 1949, pp. 547-565.

6. von Mises, R.: Bemerknung zur Hydrodynamik. Zeitschrift für Angewandte Mathematik und Mechanik, vol. 7, no. 6, Dec. 1927, pp. 425-431.

7. von Kármán, Th., and Tsien, H. S.: Boundary Layer in Compressible Fluids. Jour. Aero. Sci., vol. V, no. 6, Apr. 1938, pp. 227-232.

8. Bloom, Martin: Boundary Layers with Variable Heat Capacity on Nonisothermal Surfaces. Jour. Aero. Sci., vol. 20, no. 10, Oct. 1953, p. 719.

9. Pohlhausen, E.: Der Warmeaustausch Zwischen Festen Korpern und Flussigkeiten mit Kleiner Reibung und Kleiner Warmeleitung. Zeitschrift für Angewandte Mathematik und Mechanik, vol. 1, no. 2, 1921, pp. 115-121.

10. Low, George M.: The Compressible Laminar Boundary Layer with Fluid Injection. NACA TN 3404, 1955.

11. Tollmien, Walter: Calculation of Turbulent Expansion Processes. NACA TM 1085, 1945.

12. Gooderum, Paul B., Wood, George P., and Brevoort, Maurice, J.: Investigation with an Interferometer of the Turbulent Mixing of a Free Supersonic Jet. NACA Rep. 963, 1950.

TABLE I.- VELOCITY FUNCTION $u_*(\zeta)$ AND y DISTANCE FUNCTION $\eta(\zeta)$

ζ	u_*	η	ζ	u_*	η
-1.233	0.000	$-\infty$	1.0	0.838	0.700
-1.23	.0019	-5.22	1.1	.855	.755
-1.22	.0081	-3.87	1.2	.870	.813
-1.21	.0143	-3.41	1.3	.884	.870
-1.20	.0205	-3.12	1.4	.896	.928
-1.19	.0267	-2.91	1.5	.908	.981
-1.18	.033	-2.74	1.6	.919	1.036
-1.17	.039	-2.60	1.7	.928	1.090
-1.16	.045	-2.48	1.8	.937	1.144
-1.15	.051	-2.37	1.9	.945	1.200
-1.14	.057	-2.28	2.0	.952	1.250
-1.13	.063	-2.20	2.1	.958	1.302
-1.12	.069	-2.12	2.2	.964	1.354
-1.11	.075	-2.10	2.3	.969	1.406
-1.10	.081	-1.990	2.4	.973	1.460
-1.0	.139	-1.522	2.5	.977	1.509
-.9	.194	-1.218	2.6	.980	1.560
-.8	.247	-.991	2.7	.983	1.611
-.7	.297	-.806	2.8	.986	1.661
-.6	.345	-.650	2.9	.988	1.715
-.5	.391	-.514	3.0	.990	1.763
-.4	.434	-.393	3.1	.992	1.813
-.3	.475	-.283	3.2	.993	1.864
-.2	.515	-.182	3.3	.994	1.914
-.1	.552	-.088	3.4	.995	1.964
0	.587	0	3.5	.996	2.01
.1	.620	.083	3.6	.997	2.06
.2	.651	.162	3.7	.997	2.11
.3	.680	.237	3.8	.998	2.16
.4	.708	.309	3.9	.998	2.21
.5	.733	.378	4.0	.998	2.27
.6	.758	.445	4.1	.999	2.32
.7	.780	.510	4.2	.999	2.37
.8	.801	.574	4.3	.999	2.42
.9	.820	.638	4.4	.999	2.47
			4.5	.999	2.52
			4.6	1.000	2.57

TABLE II.- ENTHALPY-DISTRIBUTION FUNCTIONS

(a) $g_1(\zeta)$

ζ	Pr = 0.1	Pr = 0.25	Pr = 0.5	Pr = 0.72	Pr = 1.0	Pr = 1.5	Pr = 2.0	Pr = 10
-1.233	1.000	1.000	1.000	1.000	1.000	1.000	1.000	1.000
-1.23	.598	.850	.967	.991	.998	1.000	1.000	1.000
-1.22	.527	.779	.931	.974	.992	.999	1.000	1.000
-1.21	.500	.746	.909	.961	.986	.998	1.000	1.000
-1.20	.482	.722	.891	.949	.980	.996	.999	1.000
-1.19	.468	.704	.876	.938	.973	.994	.998	1.000
-1.18	.457	.688	.863	.928	.967	.991	.998	1.000
-1.17	.448	.675	.850	.919	.961	.989	.997	1.000
-1.16	.440	.663	.839	.910	.955	.986	.995	1.000
-1.15	.433	.652	.829	.901	.949	.983	.994	1.000
-1.14	.426	.642	.819	.893	.943	.980	.993	1.000
-1.13	.420	.633	.810	.885	.937	.977	.991	1.000
-1.12	.415	.624	.801	.877	.931	.974	.989	1.000
-1.11	.410	.616	.792	.870	.925	.970	.988	1.000
-1.1	.405	.609	.784	.863	.919	.966	.986	1.000
-1.0	.371	.550	.716	.797	.861	.926	.958	1.000
-.9	.347	.508	.662	.740	.806	.878	.921	1.000
-.8	.329	.475	.616	.689	.753	.828	.877	.998
-.7	.315	.447	.576	.642	.703	.776	.826	.992
-.6	.302	.422	.540	.600	.655	.723	.771	.976
-.5	.291	.400	.507	.561	.609	.671	.715	.944
-.4	.281	.380	.477	.524	.566	.619	.657	.887
-.3	.272	.362	.449	.489	.525	.568	.600	.806
-.2	.264	.345	.423	.457	.486	.520	.544	.704
-.1	.256	.329	.398	.426	.449	.474	.491	.589
0	.248	.315	.375	.397	.413	.430	.440	.473
.1	.241	.301	.353	.369	.380	.388	.392	.363
.2	.235	.287	.333	.344	.349	.350	.346	.267
.3	.229	.275	.313	.319	.320	.313	.304	.187
.4	.223	.263	.295	.297	.292	.280	.265	.125
.5	.217	.252	.277	.275	.267	.248	.230	.080
.6	.211	.241	.260	.255	.243	.220	.199	.049
.7	.206	.230	.244	.236	.220	.194	.171	.029
.8	.201	.220	.229	.217	.199	.170	.145	.016
.9	.196	.210	.215	.200	.180	.148	.123	.009
1.0	.191	.200	.201	.184	.162	.129	.103	.005
1.1	.186	.191	.188	.169	.145	.111	.086	.003
1.2	.182	.183	.176	.155	.130	.096	.072	.001
1.3	.177	.174	.164	.141	.116	.082	.059	.001
1.4	.173	.166	.153	.129	.104	.070	.048	0
1.5	.168	.158	.142	.118	.092	.060	.039	0
1.6	.164	.150	.132	.107	.081	.050	.032	0
1.7	.160	.143	.123	.097	.072	.042	.026	0
1.8	.156	.136	.114	.088	.063	.035	.020	0
1.9	.152	.129	.105	.079	.055	.029	.016	0
2.0	.148	.122	.097	.071	.048	.024	.013	0
2.1	.144	.115	.090	.064	.042	.020	.010	0
2.2	.140	.109	.083	.058	.036	.016	.008	0
2.3	.136	.103	.076	.052	.031	.013	.006	0
2.4	.133	.097	.070	.046	.027	.011	.004	0
2.5	.129	.091	.064	.041	.023	.009	.003	0
2.6	.126	.086	.058	.036	.020	.007	.003	0
2.7	.122	.081	.053	.032	.017	.006	.002	0
2.8	.119	.075	.048	.028	.014	.004	.001	0
2.9	.115	.070	.044	.025	.012	.003	.001	0
3.0	.112	.066	.040	.022	.010	.003	.001	0
3.1	.109	.061	.036	.019	.008	.002	.001	0
3.2	.105	.057	.033	.017	.007	.002	0	0
3.3	.102	.053	.029	.014	.006	.001	0	0
3.4	.099	.049	.026	.013	.005	.001	0	0
3.5	.096	.045	.024	.011	.004	.001	0	0
3.6	.093	.041	.021	.009	.003	.001	0	0
3.7	.090	.038	.019	.008	.003	0	0	0
3.8	.087	.034	.017	.007	.002	0	0	0
3.9	.085	.031	.015	.006	.002	0	0	0
4.0	.082	.028	.013	.005	.001	0	0	0
4.1	.079	.025	.012	.004	.001	0	0	0
4.2	.076	.022	.010	.004	.001	0	0	0
4.3	.074	.020	.009	.003	.001	0	0	0
4.4	.071	.017	.008	.003	.001	0	0	0
4.5	.069	.015	.007	.002	0	0	0	0

TABLE II.- ENTHALPY-DISTRIBUTION FUNCTIONS - Concluded

(b) $g_2(\zeta)$

ζ	Pr = 0.1	Pr = 0.25	Pr = 0.5	Pr = 0.72	Pr = 1.0	Pr = 1.5	Pr = 2.0	Pr = 10
-1.233	0	0	0	0	0	0	0	0
-1.23	.071	.045	.017	.006	.002	0	0	0
-1.22	.083	.066	.035	.018	.008	.002	.001	0
-1.21	.088	.076	.047	.027	.014	.004	.002	.001
-1.20	.091	.083	.056	.036	.020	.008	.004	.001
-1.19	.093	.088	.063	.043	.026	.011	.006	.001
-1.18	.095	.093	.070	.050	.032	.015	.008	.002
-1.17	.097	.097	.076	.056	.037	.019	.011	.003
-1.16	.099	.100	.082	.062	.043	.023	.014	.003
-1.15	.100	.103	.087	.068	.049	.028	.017	.004
-1.14	.101	.106	.092	.073	.054	.032	.020	.005
-1.13	.102	.109	.096	.078	.059	.036	.024	.006
-1.12	.103	.111	.100	.083	.064	.041	.028	.007
-1.11	.104	.114	.104	.088	.069	.046	.032	.009
-1.10	.104	.116	.108	.093	.074	.050	.036	.011
-1.0	.110	.131	.139	.131	.120	.098	.081	.040
-.9	.113	.141	.160	.161	.157	.144	.130	.070
-.8	.115	.147	.175	.183	.186	.183	.176	.110
-.7	.116	.152	.186	.199	.209	.216	.216	.163
-.6	.116	.155	.194	.211	.226	.242	.249	.229
-.5	.116	.156	.199	.219	.238	.261	.275	.303
-.4	.116	.156	.201	.224	.246	.273	.293	.375
-.3	.115	.155	.202	.226	.250	.280	.304	.437
-.2	.114	.154	.201	.225	.250	.283	.309	.480
-.1	.113	.152	.198	.223	.248	.281	.307	.495
0	.112	.149	.195	.219	.243	.275	.300	.482
.1	.110	.146	.190	.213	.236	.266	.290	.449
.2	.108	.143	.185	.207	.228	.255	.276	.403
.3	.107	.139	.180	.199	.218	.242	.259	.347
.4	.105	.135	.173	.191	.207	.227	.241	.280
.5	.103	.131	.167	.182	.196	.212	.222	.224
.6	.101	.127	.160	.173	.184	.196	.202	.177
.7	.099	.123	.152	.164	.172	.180	.182	.138
.8	.097	.119	.145	.154	.160	.163	.163	.106
.9	.095	.115	.138	.144	.148	.148	.144	.081
1.0	.093	.110	.131	.135	.136	.132	.127	.062
1.1	.091	.106	.123	.125	.124	.118	.110	.048
1.2	.089	.101	.116	.117	.113	.105	.095	.037
1.3	.087	.097	.109	.108	.103	.093	.081	.028
1.4	.085	.093	.103	.100	.093	.081	.069	.021
1.5	.083	.089	.096	.092	.084	.070	.058	.016
1.6	.081	.085	.090	.084	.075	.060	.049	.012
1.7	.079	.081	.084	.077	.067	.052	.040	.009
1.8	.077	.077	.078	.070	.059	.044	.033	.007
1.9	.075	.073	.072	.063	.052	.037	.027	.005
2.0	.073	.069	.067	.057	.046	.031	.022	.004
2.1	.071	.066	.062	.051	.040	.026	.017	.003
2.2	.069	.062	.057	.046	.035	.022	.014	.002
2.3	.068	.059	.053	.041	.030	.018	.011	.002
2.4	.066	.055	.048	.037	.026	.015	.009	.001
2.5	.064	.052	.044	.033	.023	.012	.007	.001
2.6	.062	.049	.040	.029	.019	.010	.005	.001
2.7	.061	.046	.037	.026	.017	.008	.004	0
2.8	.059	.043	.034	.023	.014	.006	.003	0
2.9	.057	.040	.031	.020	.012	.005	.002	0
3.0	.055	.038	.028	.018	.010	.004	.002	0
3.1	.054	.035	.025	.016	.008	.003	.001	0
3.2	.052	.032	.023	.014	.007	.002	.001	0
3.3	.051	.030	.020	.012	.006	.002	.001	0
3.4	.049	.028	.018	.010	.005	.001	0	0
3.5	.048	.026	.016	.009	.004	.001	0	0
3.6	.046	.023	.015	.008	.003	.001	0	0
3.7	.045	.021	.013	.007	.003	.001	0	0
3.8	.043	.020	.012	.006	.002	0	0	0
3.9	.042	.018	.010	.005	.002	0	0	0
4.0	.040	.016	.009	.004	.001	0	0	0
4.1	.039	.014	.008	.003	.001	0	0	0
4.2	.038	.013	.007	.003	.001	0	0	0
4.3	.037	.011	.006	.002	.001	0	0	0
4.4	.035	.010	.006	.002	.001	0	0	0
4.5	.034	.009	.005	.002	0	0	0	0

TABLE III.- SUPPLEMENTARY y DISTANCE FUNCTIONS

(a) $\eta_1(\zeta)$

ζ	Pr = 0.1	Pr = 0.25	Pr = 0.5	Pr = 0.72	Pr = 1.0	Pr = 1.5	Pr = 2.0	Pr = 10
-1.233	-∞	-∞	-∞	-∞	-∞	-∞	-∞	-∞
-1.23	-2.31	-3.37	-4.13	-4.41	-4.60	-4.77	-4.87	-5.08
-1.22	-1.54	-2.26	-2.84	-3.09	-3.26	-3.42	-3.53	-3.74
-1.21	-1.30	-1.91	-2.42	-2.64	-2.80	-2.96	-3.06	-3.28
-1.20	-1.15	-1.69	-2.16	-2.36	-2.52	-2.67	-2.77	-2.98
-1.19	-1.05	-1.54	-1.97	-2.16	-2.31	-2.46	-2.56	-2.77
-1.18	-.977	-1.42	-1.82	-2.00	-2.15	-2.29	-2.39	-2.60
-1.17	-.915	-1.33	-1.70	-1.87	-2.01	-2.15	-2.25	-2.46
-1.16	-.862	-1.25	-1.60	-1.77	-1.90	-2.04	-2.14	-2.34
-1.15	-.816	-1.18	-1.52	-1.67	-1.80	-1.93	-2.03	-2.24
-1.14	-.776	-1.12	-1.44	-1.59	-1.71	-1.85	-1.94	-2.15
-1.13	-.741	-1.07	-1.37	-1.52	-1.63	-1.76	-1.86	-2.06
-1.12	-.709	-1.02	-1.31	-1.45	-1.56	-1.69	-1.78	-1.99
-1.11	-.681	-.977	-1.25	-1.39	-1.50	-1.67	-1.71	-1.92
-1.1	-.655	-.937	-1.20	-1.33	-1.44	-1.56	-1.65	-1.86
-1.0	-.473	-.665	-.850	-.942	-1.02	-1.11	-1.17	-1.39
-.9	-.364	-.505	-.641	-.709	-.769	-.840	-.888	-1.09
-.8	-.287	-.392	-.496	-.547	-.591	-.645	-.683	-.857
-.7	-.227	-.308	-.386	-.424	-.456	-.497	-.526	-.674
-.6	-.179	-.240	-.298	-.325	-.350	-.380	-.401	-.520
-.5	-.139	-.184	-.227	-.246	-.264	-.285	-.300	-.389
-.4	-.104	-.136	-.167	-.180	-.193	-.207	-.217	-.278
-.3	-.074	-.096	-.117	-.125	-.133	-.141	-.147	-.184
-.2	-.047	-.060	-.073	-.078	-.082	-.086	-.089	-.108
-.1	-.022	-.028	-.034	-.036	-.038	-.040	-.041	-.047
0	0	0	0	0	0	0	0	0
.1	.020	.026	.0302	.032	.033	.034	.034	.035
.2	.039	.049	.0572	.060	.062	.063	.063	.059
.3	.056	.0697	.0815	.085	.087	.088	.088	.076
.4	.073	.0891	.103	.107	.109	.109	.108	.087
.5	.088	.107	.123	.127	.128	.128	.126	.094
.6	.102	.123	.141	.144	.145	.143	.140	.099
.7	.116	.139	.158	.160	.160	.157	.152	.101
.8	.129	.153	.173	.174	.174	.168	.162	.102
.9	.141	.166	.186	.187	.185	.178	.170	.103
1.0	.153	.178	.199	.199	.195	.186	.177	.104
1.1	.164	.190	.210	.210	.204	.193	.183	.104
1.2	.174	.201	.221	.219	.212	.199	.187	.104
1.3	.185	.211	.231	.228	.220	.205	.191	.104
1.4	.195	.221	.240	.235	.226	.209	.194	.104
1.5	.204	.230	.248	.242	.231	.212	.196	.104
1.6	.213	.238	.255	.248	.236	.215	.198	.104
1.7	.222	.246	.262	.253	.240	.218	.200	.104
1.8	.230	.253	.269	.258	.244	.220	.201	.104
1.9	.238	.260	.274	.262	.247	.222	.202	.104
2.0	.246	.267	.280	.266	.250	.223	.203	.104
2.1	.254	.273	.285	.270	.252	.224	.203	.104
2.2	.261	.279	.289	.273	.254	.225	.204	.104
2.3	.269	.285	.293	.276	.256	.226	.204	.104
2.4	.275	.290	.297	.279	.257	.227	.204	.104
2.5	.282	.295	.300	.281	.259	.227	.205	.104
2.6	.289	.299	.303	.283	.260	.227	.205	.104
2.7	.295	.303	.306	.285	.261	.228	.205	.104
2.8	.301	.307	.309	.286	.261	.228	.205	.104
2.9	.307	.311	.311	.287	.262	.228	.205	.104
3.0	.313	.314	.313	.289	.263	.228	.205	.104
3.1	.318	.318	.315	.290	.263	.228	.205	.104
3.2	.324	.321	.317	.291	.263	.229	.205	.104
3.3	.329	.323	.318	.291	.264	.229	.205	.104
3.4	.334	.326	.320	.292	.264	.229	.205	.104
3.5	.339	.328	.321	.293	.264	.229	.205	.104
3.6	.344	.330	.322	.293	.264	.229	.205	.104
3.7	.348	.332	.323	.294	.265	.229	.205	.104
3.8	.353	.334	.324	.294	.265	.229	.205	.104
3.9	.357	.336	.325	.294	.265	.229	.205	.104
4.0	.361	.337	.325	.295	.265	.229	.205	.104
4.1	.365	.338	.326	.295	.265	.229	.205	.104
4.2	.369	.340	.326	.295	.265	.229	.205	.104
4.3	.373	.341	.327	.295	.265	.229	.205	.104
4.4	.376	.342	.327	.295	.265	.229	.205	.104
4.5	.380	.342	.328	.295	.265	.229	.205	.104

TABLE III.- SUPPLEMENTARY y DISTANCE FUNCTIONS - Concluded
(b) $\eta_2(\zeta)$

ζ	Pr = 0.1	Pr = 0.25	Pr = 0.5	Pr = 0.72	Pr = 1.0	Pr = 1.5	Pr = 2.0	Pr = 10
-1.233	-∞	-∞	-∞	-∞	-0.418	-0.386	-0.372	-0.357
-1.23	-0.500	-0.520	-0.487	-.447	-.416	-.386	-.372	-.357
-1.22	-.399	-.450	-.457	-.434	-.411	-.385	-.372	-.357
-1.21	-.360	-.418	-.438	-.424	-.406	-.384	-.371	-.356
-1.20	-.334	-.395	-.423	-.414	-.401	-.382	-.370	-.356
-1.19	-.314	-.376	-.410	-.406	-.397	-.380	-.369	-.356
-1.18	-.298	-.361	-.399	-.398	-.392	-.378	-.368	-.356
-1.17	-.285	-.348	-.389	-.391	-.387	-.376	-.367	-.355
-1.16	-.273	-.336	-.380	-.384	-.382	-.373	-.366	-.355
-1.15	-.263	-.326	-.371	-.377	-.377	-.370	-.364	-.355
-1.14	-.254	-.316	-.362	-.371	-.373	-.368	-.362	-.354
-1.13	-.245	-.307	-.355	-.364	-.368	-.365	-.360	-.354
-1.12	-.238	-.299	-.347	-.358	-.363	-.362	-.358	-.353
-1.11	-.231	-.291	-.340	-.352	-.359	-.359	-.356	-.353
-1.10	-.224	-.284	-.333	-.347	-.354	-.356	-.354	-.352
-1.0	-.174	-.226	-.276	-.295	-.310	-.323	-.328	-.345
-.9	-.140	-.185	-.231	-.251	-.268	-.286	-.297	-.329
-.8	-.114	-.152	-.193	-.211	-.229	-.249	-.262	-.307
-.7	-.093	-.124	-.159	-.176	-.192	-.212	-.226	-.281
-.6	-.075	-.100	-.130	-.144	-.158	-.177	-.190	-.252
-.5	-.059	-.079	-.103	-.115	-.127	-.142	-.154	-.217
-.4	-.045	-.060	-.079	-.088	-.097	-.110	-.120	-.178
-.3	-.032	-.043	-.056	-.063	-.070	-.080	-.087	-.134
-.2	-.021	-.028	-.036	-.040	-.045	-.051	-.056	-.087
-.1	-.010	-.013	-.017	-.019	-.022	-.025	-.027	-.042
0	0	0	0	0	0	0	0	0
.1	.009	.012	.016	.018	.020	.023	.025	.038
.2	.018	.024	.031	.035	.038	.043	.047	.072
.3	.026	.034	.045	.050	.055	.062	.067	.100
.4	.034	.045	.057	.064	.070	.079	.085	.123
.5	.041	.054	.069	.077	.084	.094	.101	.140
.6	.048	.062	.080	.089	.097	.107	.115	.154
.7	.054	.070	.090	.100	.108	.120	.128	.164
.8	.060	.078	.100	.110	.119	.130	.139	.171
.9	.066	.085	.108	.119	.128	.140	.148	.177
1.0	.072	.092	.116	.127	.137	.148	.156	.181
1.1	.077	.098	.124	.135	.145	.156	.163	.185
1.2	.083	.104	.131	.142	.152	.162	.169	.187
1.3	.088	.110	.137	.148	.158	.168	.174	.189
1.4	.092	.115	.143	.154	.163	.173	.178	.190
1.5	.097	.120	.149	.159	.168	.177	.182	.191
1.6	.102	.125	.154	.164	.172	.180	.185	.192
1.7	.106	.129	.159	.169	.176	.183	.187	.192
1.8	.110	.134	.163	.173	.180	.186	.189	.193
1.9	.114	.138	.167	.176	.183	.188	.191	.193
2.0	.118	.141	.171	.179	.185	.190	.192	.193
2.1	.122	.145	.174	.182	.187	.192	.193	.194
2.2	.126	.148	.177	.184	.189	.193	.194	.194
2.3	.129	.151	.180	.187	.191	.194	.195	.194
2.4	.133	.154	.182	.189	.192	.195	.195	.194
2.5	.136	.157	.185	.191	.194	.195	.195	.194
2.6	.139	.160	.187	.192	.195	.196	.196	.194
2.7	.142	.162	.189	.194	.196	.196	.196	.194
2.8	.145	.164	.191	.195	.196	.197	.196	.194
2.9	.148	.166	.192	.196	.197	.197	.196	.194
3.0	.151	.168	.194	.197	.198	.197	.196	.194
3.1	.154	.170	.195	.198	.198	.197	.196	.194
3.2	.156	.172	.196	.199	.198	.197	.196	.194
3.3	.159	.173	.197	.199	.199	.198	.197	.194
3.4	.162	.175	.198	.200	.199	.198	.197	.194
3.5	.164	.176	.199	.200	.199	.198	.197	.194
3.6	.166	.177	.200	.200	.199	.198	.197	.194
3.7	.169	.179	.201	.201	.200	.198	.197	.194
3.8	.171	.180	.201	.201	.200	.198	.197	.194
3.9	.173	.181	.202	.201	.200	.198	.197	.194
4.0	.175	.181	.203	.202	.200	.198	.197	.194
4.1	.177	.182	.203	.202	.200	.198	.197	.194
4.2	.179	.183	.203	.202	.200	.198	.197	.194
4.3	.181	.183	.204	.202	.200	.198	.197	.194
4.4	.183	.184	.204	.202	.200	.198	.197	.194
4.5	.184	.184	.204	.202	.200	.198	.197	.194

TABLE IV.- COMPARISON OF INDEPENDENT METHODS OF CALCULATING RECOVERY FACTOR AND HEAT-TRANSFER RATE

Pr	Recovery Factor		Heat Transfer	
	(a) r from eq. (42) $=F_2(\zeta_d)+\frac{4Pru_{*o}^2u_{*o}'}{\left(4u_{*o}u_{*o}'\right)^{Pr}}F_1(\zeta_d)$	(b) r from eq. (A7) $=F_2(\zeta_d)+\frac{I_2(0)}{I_1(0)}$	(c) $\frac{\bar{q}_w\sqrt{Re/C}}{\rho_e u_e(h_{aw}-h_w)}$ from eq. (43) $=\frac{\left(4u_{*o}u_{*o}'\right)^{Pr}}{PrF_1(\zeta_d)}$	(d) $\frac{\bar{q}_w\sqrt{Re/C}}{\rho_e u_e(h_{aw}-h_w)}$ from eq. (A8) $=I_1(0)$
0.1	0.361	0.360	0.833	0.836
.25	.504	.503	.674	.674
.5	.712	.713	.527	.525
.72	.849	.849	.458	.456
1.0	1.000	1.000	.399	.398
1.5	1.228	1.227	.334	.334
2.0	1.424	1.422	.293	.293
10.0	3.27	3.40	.135	.136

TABLE V.- FUNCTIONS APPEARING IN EQUATIONS FOR GAS INJECTION

ζ_1	Pr = 0.5		Pr = 0.72		Pr = 1.0	
	I_1	I_2	I_1	I_2	I_1	I_2
-1.233	0.000	0.000	0.000	0.000	0.000	0.000
-1.2	.002	.002	.001	.001	.000	.000
-1.1	.019	.013	.011	.010	.006	.006
-1.0	.044	.031	.028	.025	.017	.019
-.9	.076	.055	.051	.047	.033	.039
-.8	.112	.083	.080	.074	.055	.065
-.7	.152	.116	.113	.106	.082	.097
-.6	.196	.153	.151	.144	.115	.134
-.5	.244	.194	.193	.186	.151	.178
-.4	.295	.241	.239	.233	.193	.226
-.3	.349	.291	.288	.285	.238	.279
-.2	.405	.346	.341	.341	.288	.337
-.1	.464	.405	.397	.402	.341	.400
0	.525	.468	.456	.467	.398	.467

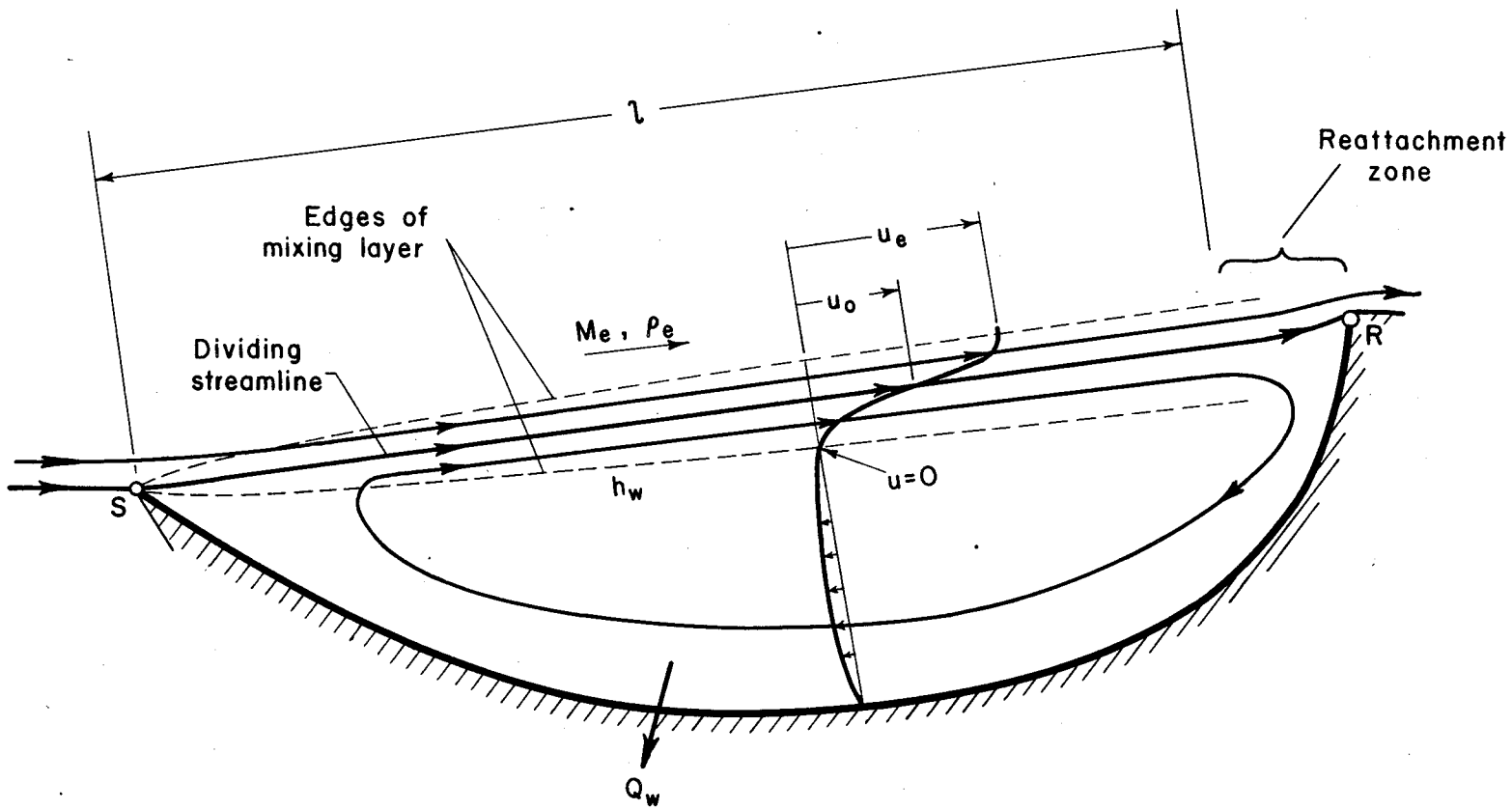

Figure 1.–Sketch of separated flow field (vertical scale expanded).

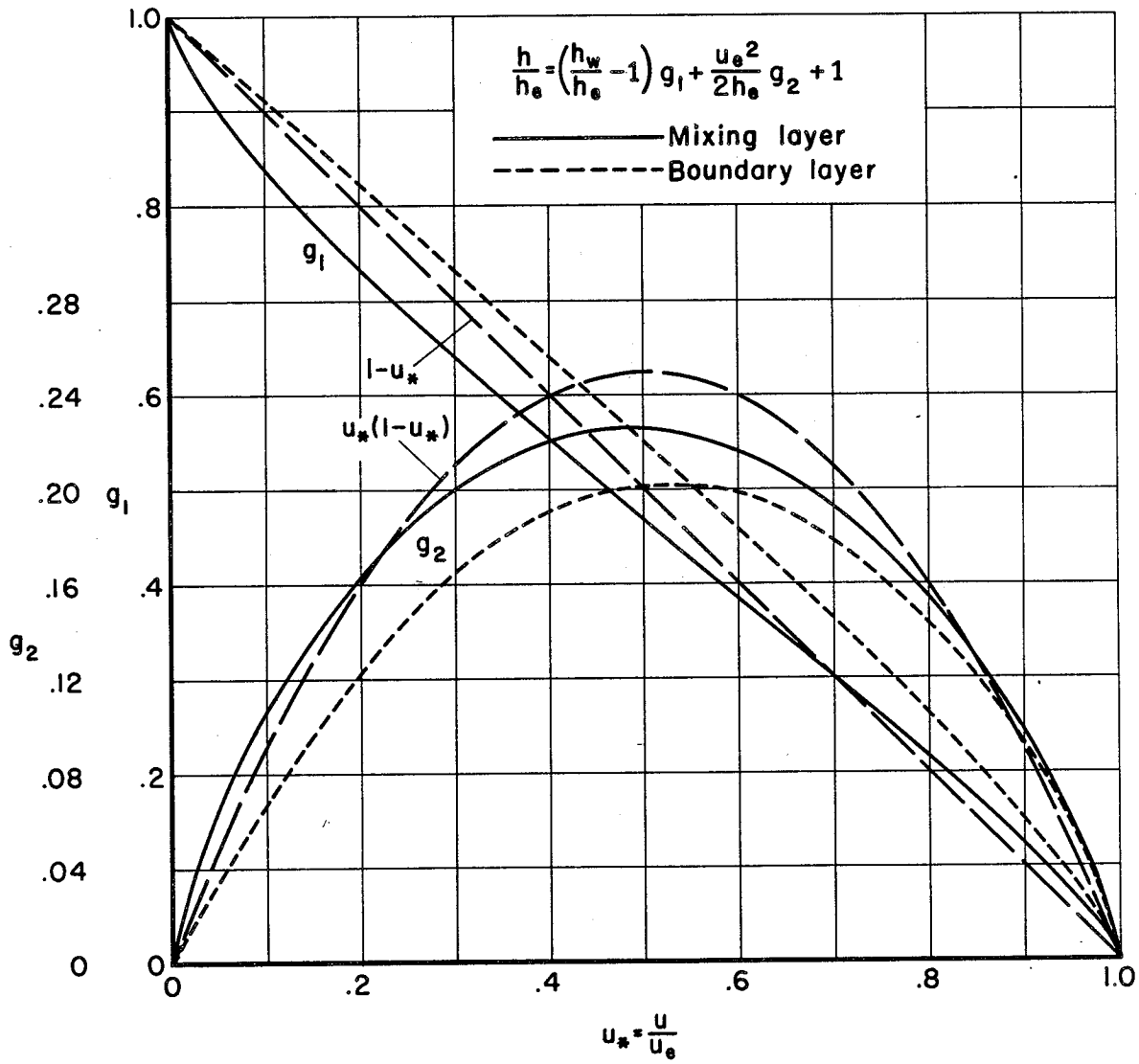

Figure 2.—Enthalpy-velocity functions for separated laminar mixing layer and for laminar boundary layer; $P_r=0.72$.

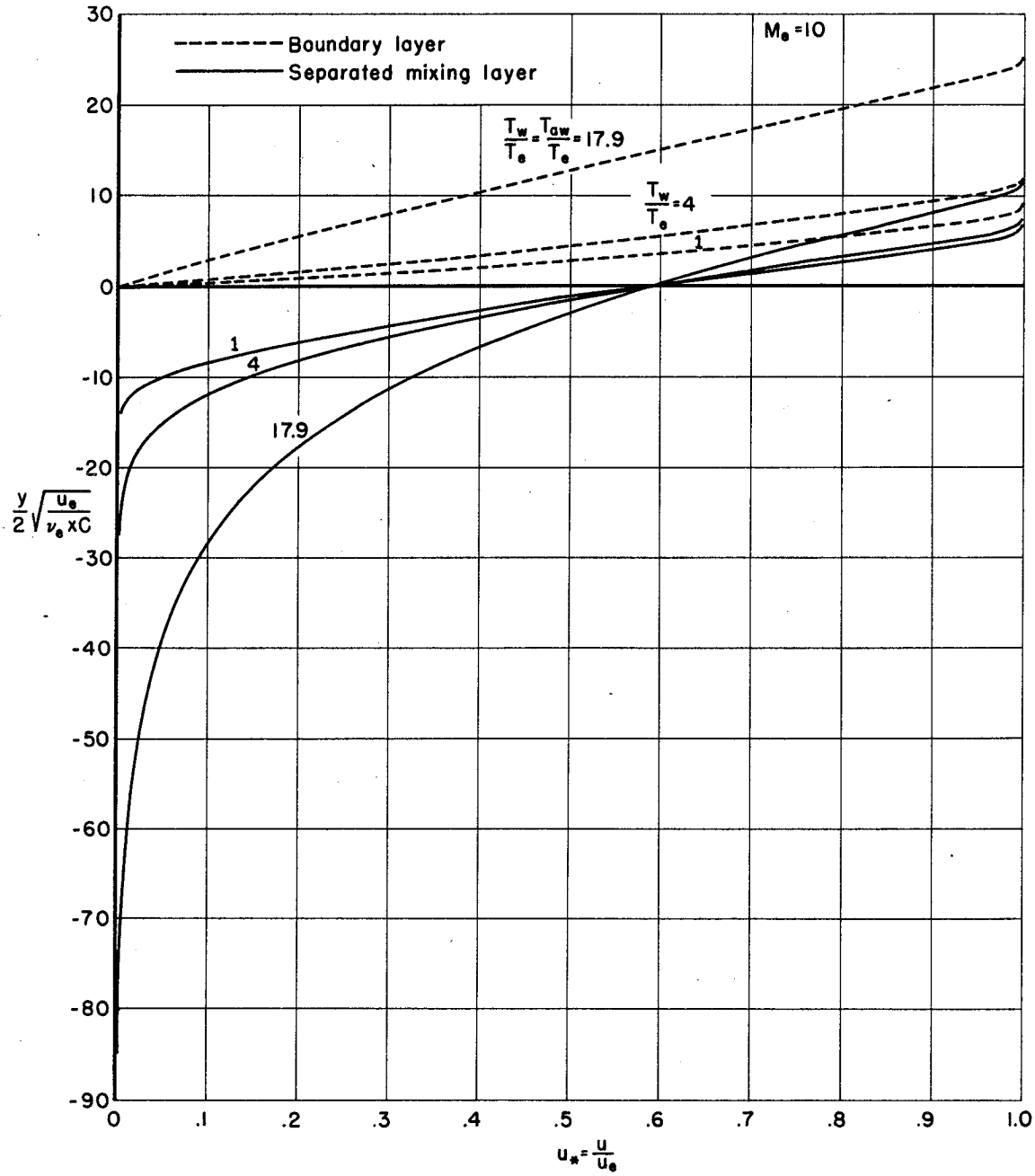

Figure 3.—Velocity profiles in separated laminar mixing layer and in laminar boundary layer for various wall temperatures; M_e=10, P_r=0.72.

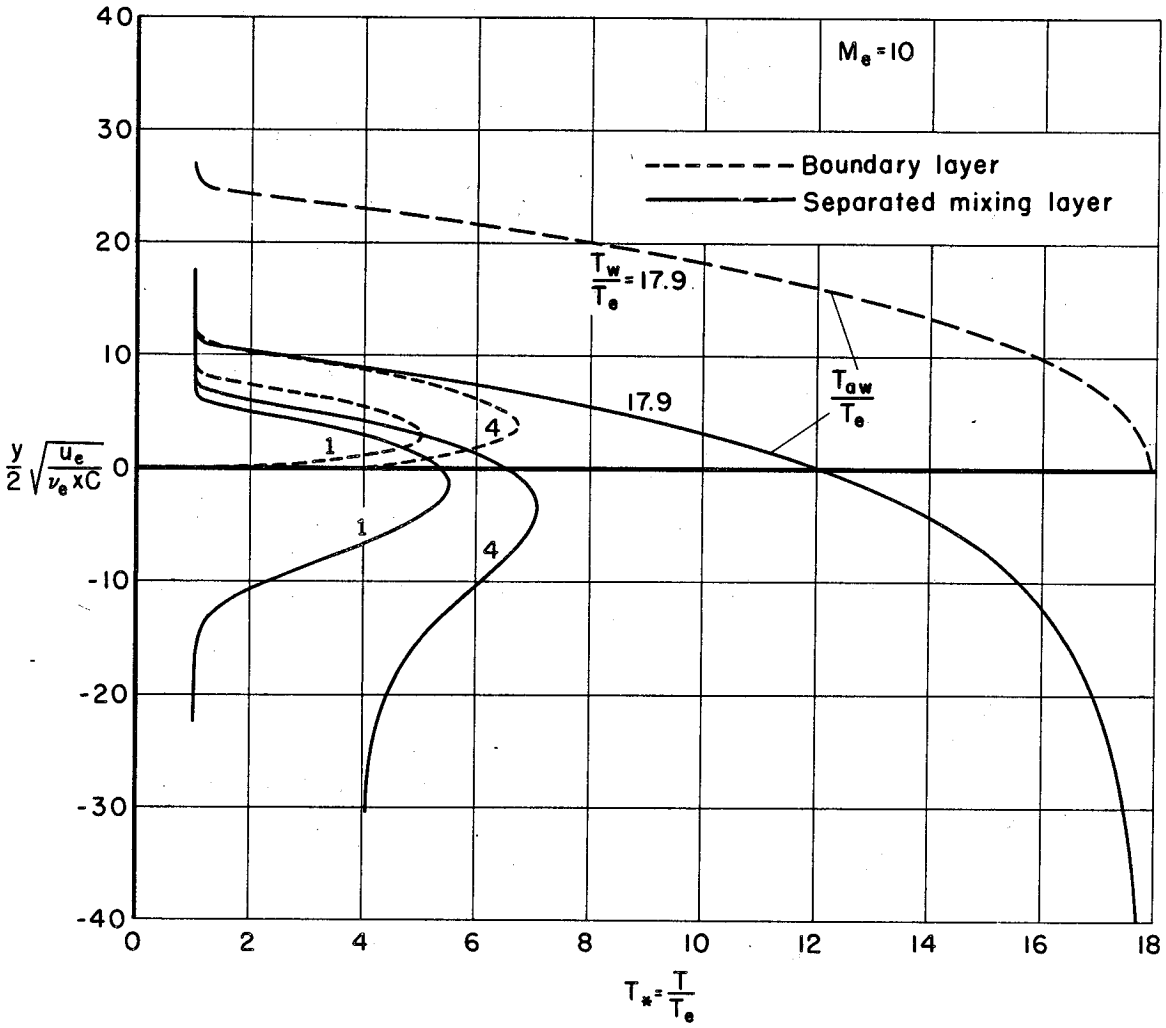

Figure 4.—Temperature profiles in separated mixing layer and in laminar boundary layer for various wall temperatures; $M_e = 10$, $P_r = 0.72$.

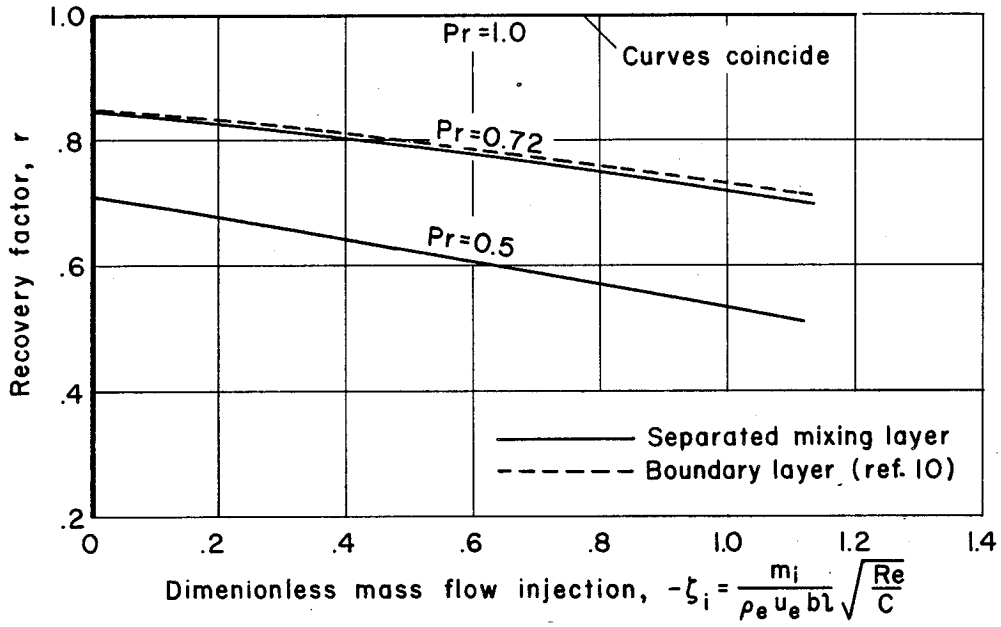

Figure 5.– Effect of mass injection on recovery factor.

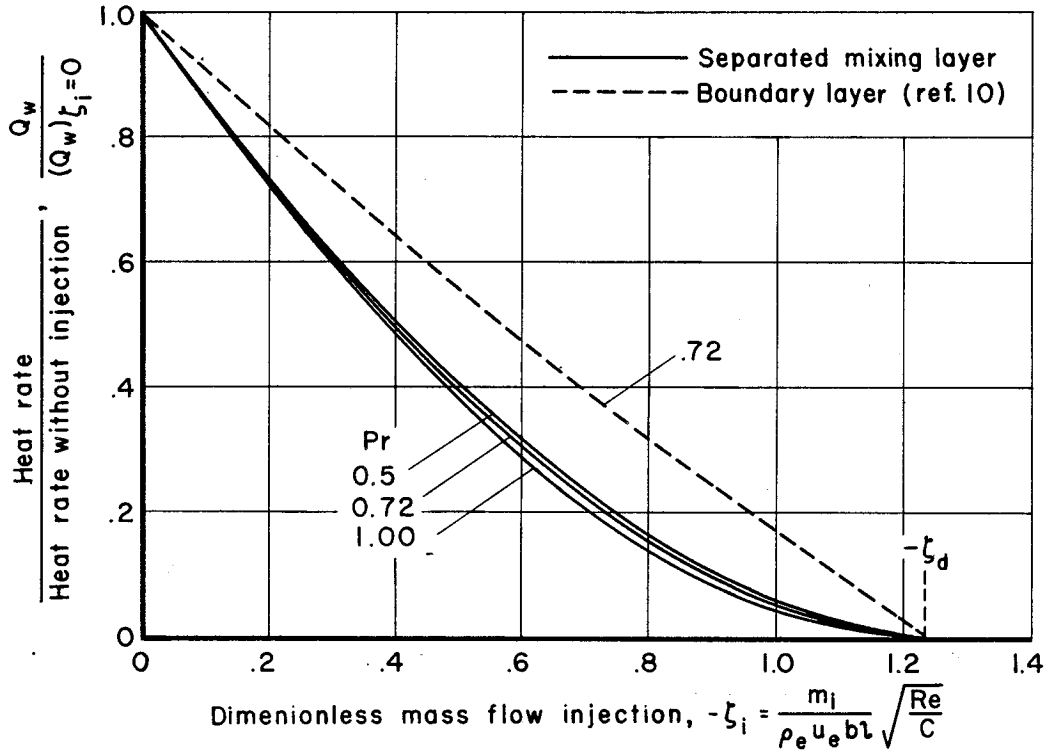

Figure 6.—Effect of mass injection on heat transfer for case $h_w/h_e=1$ (also applies to case $M_e \to \infty$ for arbitrary h_w).